Envelope Glycoprotein gB of Kaposi's Sarcoma-Associated Herpesvirus Is Essential for Egress from Infected Cells

Harinivas H. Krishnan,[1] Neelam Sharma-Walia,[1,3] Ling Zeng,[1] Shou-Jiang Gao,[2] and Bala Chandran[1,3]*

Department of Microbiology, Molecular Genetics and Immunology, The University of Kansas Medical Center, Kansas City, Kansas[1]; Department of Pediatrics, The University of Texas Health Science Center at San Antonio; San Antonio, Texas[2]; and Department of Microbiology and Immunology, Chicago Medical School, RFUMS, North Chicago, Illinois[3]

Kaposi's sarcoma-associated herpesvirus (KSHV) envelope glycoprotein gB interacts with cell surface heparan sulfate (HS) and α3β1 integrin and plays roles in the initial binding and entry into the target cells and in the induction of preexisting host cell signal pathways. To define gB function further, using a bacterial artificial chromosome (BAC) system carrying the KSHV genome (BAC36wt-KSHV), we constructed a recombinant virus genome with the gB open reading frame (ORF) deleted by replacing a 2-kb gB ORF with a 1.3-kb Kan^r gene. Stable 293T cells carrying BAC36wt-KSHV and ΔgBBAC36-KSHV genomes were generated. Transcript analyses and immunoprecipitation reactions confirmed the absence of gB in the 293T-ΔgBBAC36 cells. When monolayers of 293T-BAC36wt and 293T-ΔgBBAC36 cells were induced with tetradecanoylphorbol-13-acetate, infectious virus was detected only from the 293T-BAC36wt cell supernatants. No significant amount of DNase I-resistant viral DNA was detected in the supernatants of 293T-ΔgBBAC36 cells. BAC36wt-KSHV infected the target cells, and in contrast, no viral DNA and transcripts could be detected in cells infected with ΔgBBAC36-KSHV. Electron microscopy of 293T-ΔgBBAC36 cells revealed capsids in the nuclei, cytoplasmic vesicles with core-containing capsids, and occasional enveloped virions in the cytoplasm. However, enveloped virus particles were observed in the extracellular compartments of 293T-BAC36wt cells only and not in 293T-ΔgBBAC36 cells. Transfection of 293T-ΔgBBAC36 cells with plasmid expressing full-length gB restored the recovery of infectious KSHV in the supernatant. These results suggest that, besides its role in virus binding and entry into the target cells, KSHV gB also plays a role in the maturation and egress of virus from the infected cells.

Kaposi's sarcoma-associated herpesvirus (KSHV), or human herpesvirus 8, a lymphotropic oncogenic virus, has been implicated in the pathogenesis of Kaposi's sarcoma (13); body cavity-based B-cell lymphoma (BCBL), or primary effusion lymphoma (10); and some forms of multicentric Castleman's disease (48, 49, 52). KSHV is a member of the gamma-2 herpesvirus family, and its ~160-kb genome shows homologies with gamma-1 Epstein-Barr virus (EBV) and gamma-2 herpesvirus saimiri. KSHV possesses more than 90 open reading frames (ORFs), some of which are designated ORFs 4 to 75 by their homology to herpesvirus saimiri ORFs (40, 47). Besides possessing many genes shared by other herpesviruses, the KSHV genome also possesses genes unique to KSHV, which are designated with the prefix K (48, 49).

In vivo, KSHV DNA and transcripts have been detected in human B cells, macrophages, keratinocytes, endothelial cells, and epithelial cells (16, 17, 35, 55, 61). KSHV infects a variety of human and nonhuman cells in vitro. These include human B, macrophage, endothelial, fibroblast, keratinocyte, and epithelial cells (1, 2, 3, 7, 8, 15, 18, 26, 36, 46, 56, 57); owl monkey kidney cells; baby hamster kidney fibroblast cells; Chinese hamster ovary cells; and primary embryonic mouse fibroblast cells (1, 2, 5, 16, 25, 35, 38). Even though most of the herpesviruses initiate the lytic cycle soon after infection, KSHV infection of cultured cells results only in the establishment of latency (45). The infected cells do not support the serial passage of KSHV, and the viral genome is lost during successive passages (21, 46). Our recent studies show that in vitro KSHV infection is characterized by the expression of latency-associated ORF 73, 72, and K13 genes and transient expression of a very limited number of early lytic genes, such as ORFs 50, K5, and K8 and v-IRF2 (25).

Similar to other herpesviruses, KSHV encodes many glycoproteins, some of which are conserved herpesvirus glycoproteins. Open reading frames 8, 22, 47, 39, and 53 encode glycoproteins gB, gH, gL, gM, and gN, respectively (12, 47). KSHV also encodes additional glycoproteins, such as gpK8.1A, gpK8.1B, K1, K14, and K15, that are expressed during lytic replication (47). Studies have shown that gB, gH/gL, gM/gN, and gpK8.1A are virion envelope-associated glycoproteins (12, 24, 31, 37, 47). KSHVgB and gpK8.1A interact with cell surface heparan sulfate molecules (3, 6, 58, 59). KSHV gB possesses the integrin-interacting RGD (Arg-Gly-Asp) amino acid motif in the extracellular domain (30, 32). KSHV infection of target cells could be significantly inhibited by rabbit anti-KSHV gB antibodies, RGD peptide, and antibodies against the α3 and β1 and soluble α3β1 integrins (2). Anti-KSHV antibodies also

* Corresponding author. Mailing address: Department of Microbiology and Immunology, Chicago Medical School, 3333 Green Bay Rd., North Chicago, IL 60064. Phone: (847) 578-8822. Fax: (847) 578-3349. E-mail: bala.chandran@rosalindfranklin.edu.

TABLE 1. Primers used for PCR and amplified product lengths

Primer	Name	Sequence	Product length (bp)
A	ΔgB Kan^{r}F	CTT TTT CGG TTC AAC CTG GAG CAG ACG TGC CCA GAC ACC AAA GAC AAG TAC CAC CAA GAA GGA ATT TTA CTG TAT CTG ACA AGG GAA ACG CAA G C	1,953
B	ΔgB Kan^{r}R	AAT AAA ATT TAT GAA TCC GGT AAC CAA TGA GCC ACA TAG AGT GAC CAC GCT GCT GGC CAC GTT CAC CAC CGT TAA GGA GAA AAT ACC GCA TCA GGA A	
C	ΔgB int F	ACT TCC ACA CAA CAG GCG GAC TCT A	808
D	ΔgB int R	GTC TCC AGG TCA AAC ACG CTA CTC G	
E	ΔgB flank F	TCC AGT TCC CCC ACA CCC CCA GGA T	2,284
F	ΔgB flank R	GCA TTC CCA GCA GGA TGT TTT TGA T	

immunoprecipitated the virus α3-β1 complex, and overexpression of human α3 integrins in CHO cells increased the infectivity of the virus (2). Radiolabeled virus binding studies suggested that KSHV uses α3β1 integrin as one of the cellular receptors for entry into target cells (2). Using a KSHV ORF 50-dependent reporter 293T cell line, Inoue et al. (22) reported the inability of soluble α3β1 integrin and RGD peptides to block the infectivity of KSHV. However, in that study, virus was centrifuged with cells in the presence of polybrene, which may account for the apparent discrepancy. Polybrene is a positively charged cation that can complex with the virus envelope and bypass the need for receptors (28). This property of Polybrene is the basis for its use to increase the infectivity of many viruses and to deliver nucleic acid for gene therapy (28). The nature of another receptor(s) recognized by KSHV and the glycoproteins involved needs to be evaluated further.

After ligand interactions with integrins, numerous signaling molecules, including FAK, c-Src, and p130^{Cas}; and cytoskeletal proteins, like talin, paxillin, vinculin, and α-actin, assemble into aggregates on each side of the membrane called focal adhesions (FAs) (19). FAK is a nonreceptor protein-tyrosine kinase that localizes with vinculin at the FAs, and FAK activation is the first step necessary for outside-in signaling by integrins. Early during infection, KSHV induces the phosphorylation of FAK, leading to the activation of Src, phosphatidylinositol 3-kinase (PI-3K), protein kinase C-ζ (PKC-ζ), Rho GTPases, and the extracellular signal-regulated kinase (ERK) (38). Using soluble gB, we have demonstrated the ability of gB to mediate extensive cytoskeletal rearrangement in the target cells via the induction of a FAK–Src–PI-3K–Rho GTPase signal pathway (50). Examination of viral DNA entry suggests a role for PI-3K in KSHV entry into the target cells and a role for PKC-ζ–MEK and ERK at a post-viral-entry stage of infection (38, 50). Rabbit anti-gB antibodies inhibited FAK induction and the subsequent activation of PI-3K–PKC-ζ–MEK–ERK pathways during virus infection (2, 38). These data suggest that gB plays an important role in KSHV binding and entry into the target cells, as well as in the induction of host cell preexisting signal pathways facilitating entry and infection.

Besides its role in binding and entry into cells, gB has also been shown to be involved in the egress of herpesviruses, such as the alpha herpesvirus, pseudorabies virus (PrV), and gamma-1 EBV (9, 23, 27, 43, 44). To further define the role of KSHV gB in infection, in the present study, a virus with gB deletion (ΔgBBAC36-KSHV) was constructed in BAC36, which carries the whole KSHV genome in a bacterial artificial chromosome backbone (62). Our results showed that ΔgB-BAC36-KSHV was defective in egress from the infected cells. Complementation of the deletion with ectopic expression of gB restored this defect. These results indicate that, in addition to its role in virus binding and entry, KSHV gB also plays a significant role in virus egress.

MATERIALS AND METHODS

Cells. KSHV-carrying human B cells (BCBL-1) were cultured in RPMI 1640 (Gibco BRL, Grand Island, New York) medium with 10% heat-inactivated fetal bovine serum (FBS; HyClone, Logan, Utah), 2 mM L-glutamine, and antibiotics (1, 2, 3, 38). 293T cells (American Type Culture Collection) and human foreskin fibroblasts (HFF) were cultured in Dulbecco's modified Eagle's medium (DMEM; Gibco BRL) supplemented with 10% FBS, 2 mM L-glutamine, and antibiotics. Human microvascular dermal endothelial cells (HMVEC-d; CC-2543; Clonetics) were maintained in endothelial basal medium 2 (BioWhittaker, Walkersville, Maryland) and necessary growth factors provided by the manufacturer.

BCBL-KSHV. The KSHV lytic cycle was induced from the BCBL-1 cells by 20 ng/ml of 12-O-tetradecanoylphorbol-13-acetate (TPA; Sigma, St. Louis, Missouri) for 96 h. Virus from the supernatant was collected and purified, and different batches of viruses were pooled according to procedures described before (38). DNA was extracted from the virions, and copy numbers were quantitated by real-time DNA PCR using primers amplifying the ORF 73 gene of KSHV (25).

Antibodies. Rabbit polyclonal antibodies against KSHV ORF 73 (LANA-1) (2, 36, 57) and full-length gB proteins (58) and monoclonal antibodies against KSHV-gpK8.1A and ORF 59 (11, 63) proteins were used in this study.

Construction of mutant ΔgBBAC36-KSHV. BAC36wt carrying the entire KSHV genome (62) maintained and replicated in *Escherichia coli* DH10B were grown in LB medium in the presence of 25 μg/ml chloramphenicol (Cap). Mutagenesis of ORF 8 (gB) was performed with the help of the recombination system GET (λ *gam recE recT*) (39, 42) in the plasmid pGET-rec. *E. coli* DH10B cells harboring the BAC36 genome were transformed with pGET-rec plasmid and selected with 25 μg/ml Cap and 100 μg/ml of ampicillin (Amp).

PCR primers A and B are 97 bases in length; 72 bases at the 5′ ends of these primers correspond to the gB sequence, and 25 bases at the 3′ ends correspond to the kanamycin resistance (Kan^r) gene (Table 1 and Fig. 1). An ~1.3-kb PCR fragment containing the Kan^r gene flanked on both sides by gB sequence was amplified from PCR blunt vector by these primers. PCR was carried out at an extension temperature of 68°C for 3 minutes for a total of 40 cycles using Platinum *Taq* (Invitrogen Inc.) for better fidelity of the reaction. After electrophoresis, the 1.3-kb PCR product was electroeluted from the gel, and 500 ng was electroporated at 1.8 kV, 200 Ω, and 25 μF into DH10B cells carrying BAC36wt-KSHV and pGET-rec plasmids. The electroporated cells were suspended in 1 ml of SOC medium (4a), incubated at 37°C for 3 h with shaking, and plated onto two LB agar plates containing the antibiotics Cap, Amp, and Kan at 25, 100, and 30 μg/ml concentrations, respectively. After overnight incubation at 37°C, colonies were screened for the deletion of the gB ORF by PCRs as described below. The ΔgBBAC36 plasmid with the proper deletion was prepared from overnight cultures using a Large-construct kit (QIAGEN Inc., Valencia, CA) to purify it from the pGET-rec plasmid. The purified ΔgBBAC36 genome was electroporated into electrocompetent DH10B cells (Invitrogen Inc.) to separate it from the pGET-rec plasmid and was selected in the presence of 100 and 30 μg/ml of Cap and Kan, respectively. These cells were stored in 20% glycerol at −80°C.
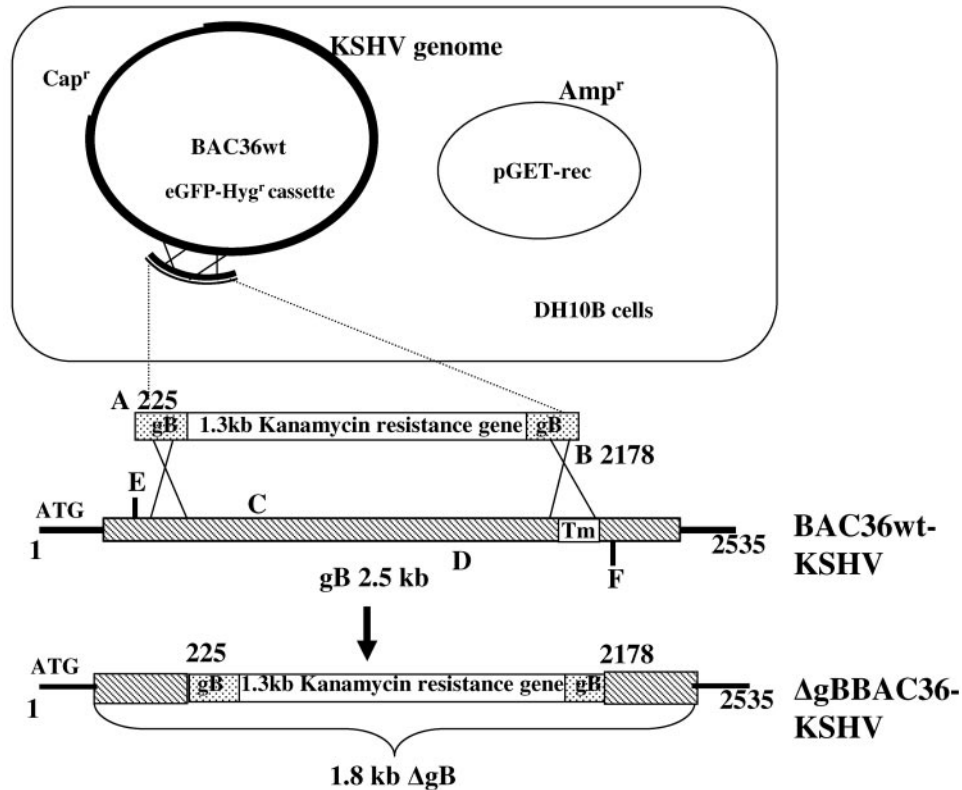
FIG. 1. Schematic diagram of KSHV gB ORF replacement with Kan[r] gene. The KSHV gB ORF is 845 aa long (2,535 bp). The ~1.3-kb Kan[r] gene flanked by gB sequence (72 bp) was PCR amplified using primer pair A and B and electroporated into DH10B cells harboring the KSHV genome in a BAC plasmid (BAC36 wt-KSHV) with the chloramphenicol resistance gene (Cap[r]) and pGET-rec plasmid with the ampicillin resistance gene (Amp[r]). Recombinants were selected with chloramphenicol, ampicillin, and kanamycin. Primers E and F amplify the gB ORF flanking the deleted region, and primers C and D amplify a region within the deleted region of the gB ORF.

Confirmation of replacement of gB by the Kan[r] gene in ΔgBBAC36-KSHV. The initial confirmation of the colonies grown on LB agar plates containing Cap, Amp, and Kan was performed by colony PCR using primer pairs A and B (Table 1 and Fig. 1 and 2). Colonies positive for the ~1.3-kb product were further screened for the absence of the ~800-bp gB fragment within the deleted region by a second round of PCR using PCR primers C and D (Table 1). A third round of PCR, recognizing sequences immediately outside primers A and B amplifying a region spanning the deleted fragment, was performed by primers E and F (Table 1) to further confirm the replacement of the 2-kb gB sequence by the 1.3-kb Kan[r] gene.

Five micrograms each of BAC36wt and ΔgBBAC36 plasmid was digested with SmaI restriction enzyme (Promega Corp., Madison, Wisconsin), electrophoresed in a 0.8% agarose gel, and transferred onto nylon membranes. Radiolabeled probes of PCR products amplified by primer sets C-D and E-F, 808 bp and 2,284 bp, respectively, were prepared by random labeling. Briefly, 200 ng of the electroeluted PCR products was subjected to polymerization with the help of Klenow fragment (New England Biolabs Inc., Beverly, Mass.) in the presence of [α-^{32}P]dCTP (Amersham Pharmacia Biotech, Piscataway, New Jersey). The radiolabeled product was purified by a nucleotide removal kit (QIAGEN Inc.). HindIII-digested λ phage DNA was also radiolabeled by similar procedures. Nylon blots were prehybridized at 60°C for 6 h in prehybridization solution (6× SSC [1× SSC is 0.15 M NaCl plus 0.015 M sodium citrate], 0.5% sodium dodecyl sulfate [SDS], 5× Denhardt's solution, and salmon sperm DNA). Radiolabeled probes were boiled for 5 min, chilled on ice, added to hybridization buffer, and incubated at 60°C overnight. Washing was performed with a series of wash buffers (2× SSC-0.5% SDS, 1× SSC-0.5% SDS, and 0.1× SSC-0.5% SDS, each twice at 60°C for 15 min), and the blots were exposed to XAR film at −70°C.

Transfection of BAC36wt and ΔgBBAC36 plasmids. Transfection of BAC36wt and ΔgBBAC36 plasmids into cells grown in six-well plates was performed using Lipofectamine 2000 reagent (Invitrogen Inc.), together with peptide enhancer (Targeting Systems, Santee, California). DNA was mixed with 500 μl of Opti-

MEM medium (Invitrogen Inc.); 10 μl of Lipofectamine 2000 and 5 μl of the peptide enhancer were mixed in another 500 μl of Opti-MEM, and both were incubated at room temperature for 5 min. The two solutions were mixed and further incubated at room temperature for another 20 min. This mixture was mixed with 1 ml of DMEM supplemented with 5% heat-inactivated FBS, 2 mM L-glutamine, and the whole mixture was added to individual wells of 293T cells in six-well plates and incubated for 12 h at 37°C and 5% CO$_2$. After 12 h, the medium was replaced with DMEM supplemented with 5% FBS and 2 mM L-glutamine and further incubated for 24 h, and the cells were observed under an inverted Nikon Eclipse TE2000U fluorescence microscope (Nikon, Melville, NY). After green fluorescent protein (GFP) detection, the cells were scraped with a rubber policeman, seeded in 24-well plates at a concentration of 1 cell/ well, and grown in the presence of 75 μg/ml of hygromycin for clonal selection of transfected cells. Different clones were selected after about 4 weeks of growth in hygromycin.

Preparation of BAC36wt and ΔgBBAC36-KSHV. 293T cells stably transfected with BAC36wt and ΔgBBAC36 genomes were grown in DMEM supplemented with 10% FBS, 2 mM L-glutamine, 100 U of penicillin/ml, and 75 μg/ml of hygromycin. The cells in 15 flasks (75 cm^2) were treated with 20 ng/ml of TPA for 96 h, and virus was purified from the supernatants according to procedures described before (38). Purified viruses were resuspended in DMEM, passed through a 0.45-μm-pore-size filter membrane to remove cellular debris, and stored at −80°C. Viral DNA copies of different batches of preparations were determined by real-time DNA PCR primers amplifying the KSHV ORF 73 gene according to procedures described before (25).

Preparation of DNA and RNA. Total DNAs from the viral stocks and cells were prepared using a DNeasy Tissue kit (QIAGEN Inc.). Monolayers of infected cells were trypsinized for 5 min at 37°C and collected with 10 ml of ice-cold DMEM. The cells were pelleted at 1,000 rpm for 10 min, washed, and resuspended in 200 μl of 1× phosphate-buffered saline (PBS), and total DNA was prepared according to the manufacturer's instructions. For the preparation of
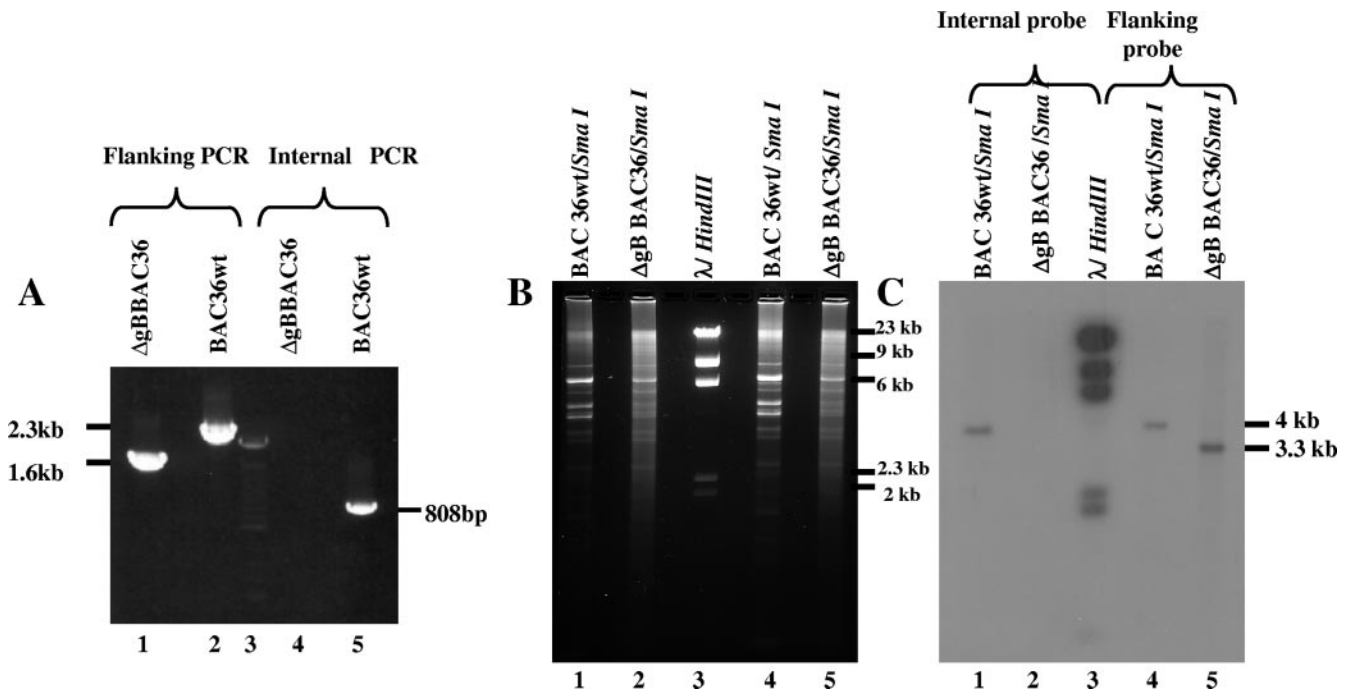
FIG. 2. (A) Confirmation of KSHV gB replacement by PCR. The BAC36wt-KSHV (lanes 2 and 5) and ΔgBBAC36-KSHV (lanes 1 and 4) genomes were amplified with flanking PCR primers E and F and internal PCR primers C and D (Fig. 1). Lane 3, molecular size markers. (B and C) Confirmation of gB deletion by Southern hybridization. BAC36wt and ΔgBBAC36-KSHV DNAs were digested with SmaI, electrophoresed, and blotted onto nylon membranes. (B) Gels were stained with ethidium bromide. (C) Radiolabeled probes of the 800-bp gB region amplified by the internal primer and the 2.3-kb gB region amplified by the flanking primers were prepared by a random-labeling method and hybridized with the membranes. Lanes 1 and 2, SmaI-digested BAC36wt and ΔgBBAC36-KSHV DNAs probed with internal fragment. Lanes 4 and 5, SmaI-digested BAC36wt and ΔgBBAC36-KSHV DNAs probed with flanking PCR probe. Lane 3, λ phage DNA digested with HindIII and probed by radiolabeled λ DNA.

DNA from intact virions, 200 μl of virus stocks was pretreated with 12 μg of DNase I for 15 min at room temperature, the reaction was stopped with EDTA followed by heat inactivation at 70°C, and DNA was prepared. Total RNA was isolated from infected or uninfected cells using an RNeasy kit as described previously (25). Target cells were infected with virus for 2 h and washed to remove unbound virus, and the cells were lysed to prepare RNA samples. RNA was also prepared from TPA-induced or uninduced 293T-BAC36wt and 293T-ΔgBBAC36 cells.

Real-time DNA PCR and reverse transcription (RT)-PCR. Copy numbers of KSHV DNA in viral stocks and in the infected cells were estimated by real-time DNA PCR according to procedures described previously (25). Briefly, total DNA was prepared using a DNeasy tissue kit (QIAGEN Inc.), and 100 ng of the DNA samples was subjected to real-time DNA PCR containing primers and Taqman probes for the detection the KSHV ORF 73 gene (25). Viral DNA copy numbers were calculated using external standards of known concentrations of ORF 73 plasmid.

Real-time RT-PCR was performed to quantitate the KSHV ORF 50, ORF 73, and ORF K8 transcripts according to the protocols described previously (25, 51). Total RNA was prepared from samples and treated with DNase I (amplification grade; Invitrogen Inc.) to remove contaminating DNA, and 250 ng of DNase I-treated RNA was used in each real-time RT-PCR with gene-specific primers and Taqman probes (25, 51). External standards containing different dilutions of known concentrations of the respective transcripts synthesized by in vitro transcription reaction (Megascript; Ambion Inc., Austin, Texas) were used to quantitate viral transcripts in the RNA samples.

RT-PCR. RT-PCRs of virus-specific genes were performed as reported previously (25). Total RNA was prepared, treated with DNase I, and converted to cDNA by a Superscript II RT-PCR system (Invitrogen Inc.) and random hexamers; 250 ng of cDNA was used in each reaction for the amplification of viral transcripts using transcript-specific primers (25). β-Actin was used as the normalization control for RNA inputs. RT-PCR products were run on a 2% agarose gel and analyzed using the Alphaimager 2000 (Alpha Innotech Corp.) gel documentation system. Amplification of DNase I-treated RNA without the RT

reaction confirmed the absence of any contaminating DNA in the cDNA samples.

Immunoprecipitation and Western blotting. 293T, 293T-BAC36wt, and 293T-ΔgBBAC36 monolayer cells were induced with 20 ng/ml of TPA. After 96 h, the cells were washed with 1× PBS, lysed with RIPA lysis buffer (50 mM Tris-HCl, pH 7.4, 150 mM NaCl, 0.1% SDS, 1% Triton X-100, 1% deoxycholate, 1 mM sodium orthovanadate [Na$_3$VO$_4$], 20 mM sodium pyrophosphate, 100 mM sodium fluoride, 10% glycerol, 1 mM EDTA, 5 μg/ml of aprotinin, 5 μg/ml of leupeptin, 5 mM benzamidine, and 1 mM phenylmethylsulfonyl fluoride), homogenized, and centrifuged at 13,000 rpm for 20 min at 4°C. Protein concentrations were estimated with the bicinchoninic acid protein assay reagent (Pierce, Rockford, Ill.). Five hundred micrograms of protein from different samples was mixed with rabbit polyclonal anti-gB or monoclonal anti-gpK8.1A antibody and rocked at 4°C overnight. Fifty microliters of protein A-Sepharose beads was added to these samples, and the mixture was rocked for 90 min at 4°C. The beads were washed four times with RIPA buffer, boiled for 5 min in lysis buffer, and tested in Western blot reactions. The membranes were blocked with 5% nonfat dry milk solution in TBST buffer (10 mM Tris-HCl, pH 7.2, 150 mM NaCl) containing 0.1% Tween 20 at room temperature for 2 h. The blots were reacted with rabbit anti-full-length gB antibodies (58) and monoclonal antibodies against gpK8.1A at 4°C overnight and washed five times with washing buffer (10 mM Tris-HCl, pH 7.2, 150 mM NaCl, 0.3% Tween 20). The blots were reacted with alkaline phosphatase-conjugated secondary antibodies (KPL, Gaithersburg, Md.) for 1 h at room temperature. The antibody reactions were performed and the bands were detected with the help of CDP-Star (Roche Diagnostics, Indianapolis, IN).

Immunoperoxidase assay. Immunoperoxidase assays to detect viral proteins were performed as described previously (25). 293T, 293T-BAC36wt, and 293T-ΔgBBAC36 cells grown in eight-well glass chamber slides were washed with 1× PBS and fixed with ice-cold acetone. The slides were incubated with 5% hydrogen peroxide solution, and then prestandardized dilutions of the primary antibodies were added to the slides and incubated at room temperature for 1 h. These slides were washed with 1× PBS and incubated with biotinylated anti-

rabbit or anti-mouse antibodies (Vectastain ABC kit; Vector Laboratories, Burlingame, Calif.), and proteins were detected with an avidin-biotin complex containing horseradish peroxidase. Diaminobenzidine was the substrate for the peroxidation reactions, and the reactions were stopped after sufficient color development. The slides were dehydrated in a series of 70 to 90% absolute ethanol, followed by xylene; sealed permanently with cytoseal; and examined under a Nikon light microscope with a digital imaging system.

Complementation of 293T-ΔgBBAC36 cells with gB-pcDNA3.1. Fifteen micrograms of gB-pcDNA3.1 plasmid was transfected into the 293T-ΔgBBAC36 cells using Lipofectamine 2000 and peptide enhancer. After 48 h, the cells were induced with 20 ng/ml of TPA for 96 h, and virus was purified from the supernatants.

Electron microscopy. Cells were induced with TPA for 96 h, washed with 1× PBS, collected with a rubber policeman, washed twice in 1× PBS, fixed with 2% glutaraldehyde, rinsed in PBS, postfixed in 1% osmium tetroxide, dehydrated in a graded series of ethanol, and embedded in Embed 812 resin. Thin sections were made and viewed under a JEOL 100CXII transmission electron microscope.

RESULTS

Construction of ΔgBBAC36-KSHV. Using the GET recombination system, we constructed the ΔgBBAC36-KSHV genome by deleting a 2-kb gB ORF region in the BAC36wt-KSHV genome (Fig. 1). The PCR primers designed for the recombination event had 72 base pairs on both ends that were homologous to gB ORF sequences, with the 5′ end of the product corresponding to nucleotide position 226 downstream to the ATG start codon, while the 3′-end homologous sequence corresponded to nucleotide position 2178. By this method, we replaced a major portion of the gB ORF, including the transmembrane domain, with a 1.3-kb Kan^r gene under its own promoter flanked on both sides with gB sequences. The purified 1.3-kb PCR product was introduced into *E. coli* DH10B harboring the BAC36wt genome and the recombination-facilitating plasmid pGET-rec (Fig. 1).

Colonies were screened by PCR for detection of the electroporated DNA fragment using primers A and B (Fig. 1). Positive colonies were screened by PCR-2 using primer set C and D amplifying a product of 808 nucleotides within the deleted 1,169- to 1,977-bp region of the gB ORF (Fig. 1). Colonies which did not amplify in PCR-2 were further screened by PCR-3 using primer set E and F recognizing gB ORF sequences just outside of primers A and B and amplifying the entire deleted region of gB (Fig. 1). A 2.3-kb region was amplified by primers E and F from the gB ORF, while in the deleted ORF, they amplified a smaller, 700-bp product. Colonies in which no product was seen in PCR-2 amplified a product of about 1.6 kb in PCR-3 compared to the 2.3-kb product from the wild-type gB, thus demonstrating the recombination event (Fig. 1 and Fig. 2A, lanes 1 and 2). Colonies demonstrating the expected results for all the three PCRs were considered to have BAC36 with the Kan^r gene replacing gB and were designated ΔgBBAC36. An approximately 2-kb region within the gB ORF was replaced with a 1.3-kb fragment expressing Kan^r, which was confirmed by amplifications of a region flanking the deleted sequence and an internal fragment. The flanking PCR amplified a 1.6-kb product from the ΔgBBAC36 genome (Fig. 2A, lane 1), while a 2.3-kb fragment was amplified from the BAC36wt genome (Fig. 2A, lane 2). A PCR which amplifies a region inside the deleted fragment did not amplify any product in ΔgBBAC36 DNA, while it amplified an 808-bp region from BAC36wt DNA (Fig. 2A, lanes 4 and 5).

E. coli DH10B cells carrying the ΔgBBAC36 genome were grown in the absence of ampicillin to cure the pGET-rec plasmids, and pure ΔgBBAC36 DNA was isolated. To confirm the proper replacement of gB with the Kan^r gene, 5 μg each of BAC36wt and ΔgBBAC36 DNAs digested with SmaI was used for hybridization experiments (Fig. 2B and C). When probed with the 808-bp radiolabeled PCR product of primers C and D, hybridization with a 4-kb fragment was observed with BAC36wt DNA; in contrast, no signal was detected with ΔgBBAC36 DNA (Fig. 2C, lanes 1 and 2). The 2.3-kb radiolabeled PCR product of primers E and F detected a 4-kb fragment in BAC36wt DNA and a 3.3-kb fragment in ΔgBBAC36 DNA (Fig. 2C, lanes 4 and 5). The detection of a smaller fragment was due to the replacement of the 2-kb gB ORF region with the 1.3-kb Kan^r gene. These experiments further confirmed the replacement of a 2-kb region of the gB ORF by a 1.3-kb Kan^r gene.

Generation of stable 293T cells carrying BAC36wt and ΔgBBAC36 genomes. To permit the induction of the lytic replicative cycle and progeny KSHV, BAC36wt and ΔgBBAC36 genome plasmid preparations were transfected into suitable cell types. The presence of a Hyg^r-enhanced green fluorescent protein (eGFP) cassette integrated into the genomes of BAC36wt and ΔgBBAC36 in between ORFs 18 and 19 enabled us to monitor the efficiency of transfection by eGFP detection, selective growth of transfected cells, and the establishment of stably transfected cell lines. Due to the characteristics of in vitro KSHV infection, such as the establishment of latent infection, the inability of infected cells to support serial passages of KSHV, and loss of the viral genome during successive passages (21), an important prerequisite for this work was the selection of suitable cells that allowed the highest transfection efficiency and successful preparation of virus stocks. Human primary endothelial cells are biologically more relevant, and HFF have also been shown to support infection (2, 38). However, since both are primary cells and do not support a large number of serial passages, they were not suitable for the establishment of stable cells. Moreover, HFF do not support lytic replication when induced by TPA (5, 55; Krishnan et al., unpublished data). We could not use TIME (telomerase-immortalized microvascular endothelial) cells due to low efficiency of transfection.

293-HEK cells are permissive for KSHV infection, and a productive lytic-cycle induction has been shown in these cells (5, 62). We initially transfected 293-HEK cells with different amounts of BAC36wt and ΔgBBAC36 plasmids, using Lipofectamine 2000 as the transfecting agent, but transfection efficiency was only about 5% and could not be increased with the use of other reagents, including peptide enhancers. However, with Lipofectamine 2000, we observed a higher transfection efficiency of up to 15% in 293T cells containing simian virus 40 large T antigen, which increased to ~20% with the addition of peptide enhancer. Transfection efficiency did not increase significantly with increasing amounts of DNA, and 1 μg of DNA was the optimum dose in these transfections.

Transiently transfected 293T cells were subcultured in 24-well plates at a concentration of 1 cell/well. Twenty-four hours after the subculture, the medium was changed and the cells were grown in the presence of 75 μg/ml of hygromycin to prepare stable transfected cells. Monolayers were formed after
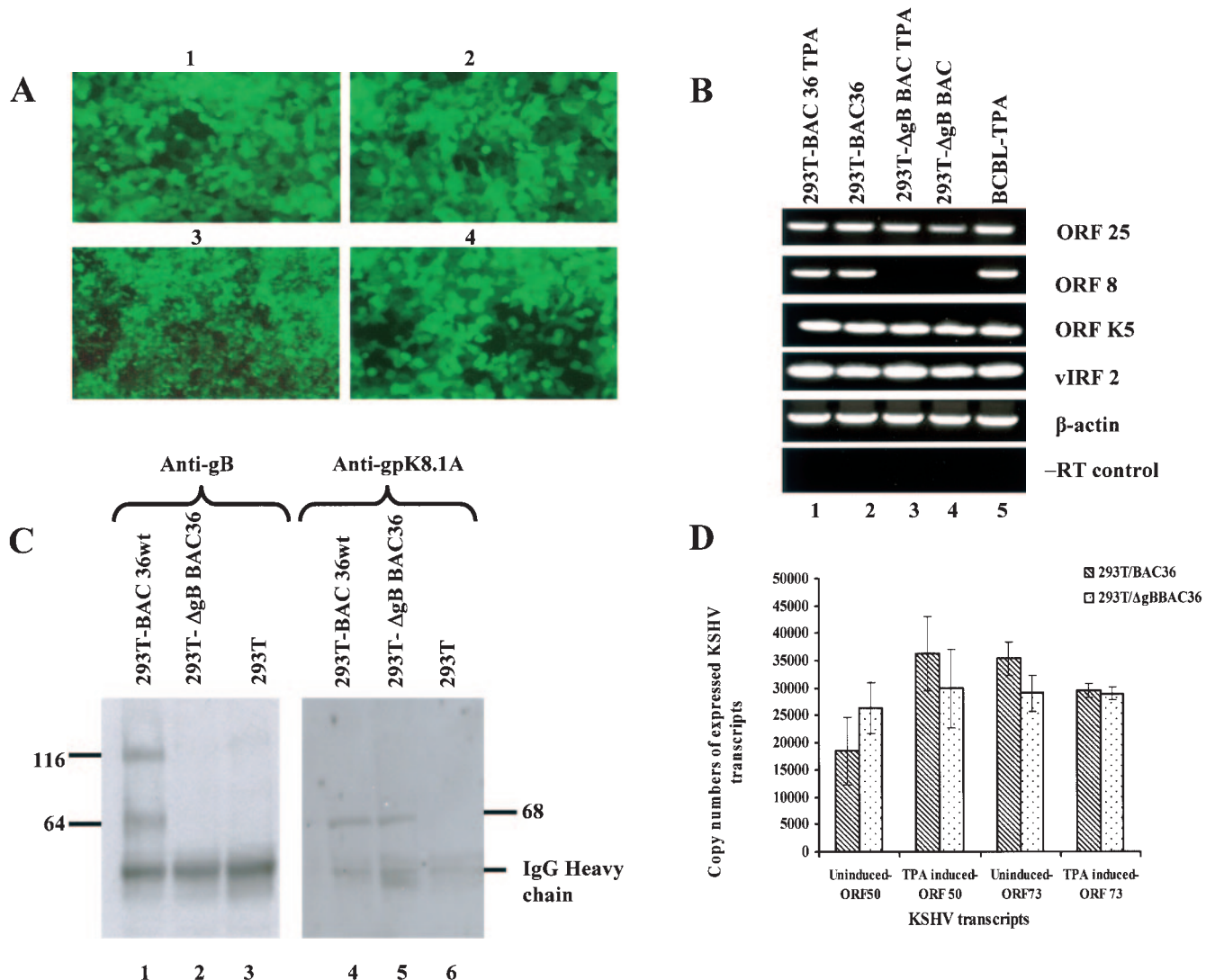
FIG. 3. (A) GFP expression in 293T cells stably transfected with BAC36wt and ΔgBBAC36-KSHV genomes. Cells were transfected with BAC36wt and ΔgBBAC36-KSHV genomes in Lipofectamine 2000 and peptide enhancer and selected with hygromycin, and clones were established. Images 1 and 2, 293T-BAC36wt-KSHV genome-containing cells. Images 3 and 4, 293T-ΔgB BAC36-KSHV genome-containing cells. Magnification, ×40. (B) RT-PCR confirmation of the absence of gB in 293T-ΔgBBAC36 cells. Total RNAs from uninduced or TPA-induced 293T-BAC36wt and 293T-ΔgBBAC36 cells were prepared, DNase treated, and used for cDNA synthesis. cDNA (250 ng) was used in each PCR and tested for KSHV ORFs 25, 8, and K5 and vIRF2. The RNA quantity was assessed by the amplification of β-actin transcript. Absence of contaminating DNA in the samples was tested by reverse transcriptase-negative (−RT) control reactions. (C) Immunoprecipitation confirmation of the absence of gB in 293T-ΔgBBAC36-KSHV cells. Lysates from 293T-BAC36wt and 293T-ΔgBBAC36 cells induced with TPA for 96 h were immunoprecipitated with rabbit anti-gB polyclonal antibodies (lanes 1 to 3) and anti-gpK8.1A monoclonal antibodies (lanes 4 to 6). Immuno-precipitated proteins were immunoblotted with the respective antibodies and tested with alkaline phosphatase-conjugated secondary antibodies. The numbers indicate the molecular masses (in kilodaltons) of the gB and gpK8.1A proteins detected. (D) Quantitation of KSHV ORF 50 and 73 transcripts by real-time RT-PCRs. Uninduced or TPA-induced 293T-BAC36wt and 293T-ΔgBBAC36 cells were collected, and total RNA was prepared, DNase treated, and used for cDNA synthesis. DNase-treated RNA (250 ng) was subjected to real-time RT-PCR with ORF 73 and 50 gene-specific primers and Taqman probes. Known concentrations of DNase-treated in vitro-transcribed ORF 50 and ORF 73 transcripts were used in a real-time RT-PCR to construct a standard graph from which the absolute copy numbers of viral transcripts were calculated and normalized to GAPDH (glyceraldehyde-3-phosphate dehydrogenase) transcript copies used as the internal control. Each reaction was done in duplicate, and each bar represents the average ± standard deviation of three experiments.

about 4 weeks, and all cells were positive for GFP expression. Clones were isolated, grown further in 25-cm² flasks, and tested by real-time DNA PCR for the KSHV ORF 73 gene and for the deletion of the gB gene (data not shown). GFP expression was observed in all the cells of stable cultures (Fig. 3A, 1 to 4). Relatively stronger GFP signal was observed in ~10% of

uninduced cells, which could represent cells spontaneously entering the lytic cycle.

KSHV lytic transcript analyses confirm gB deletion in 293T-ΔgBBAC36 cells. Stably transfected cells in 75-cm² flasks were induced with TPA, and total RNA was isolated from induced and uninduced cells, treated with DNase I, and analyzed by

RT-PCR for KSHV lytic-cycle transcripts. No gB (ORF 8) transcript was detected in 293T-ΔgBBAC36 cells (Fig. 3B, lanes 3 and 4), while it could be easily detected in the 293T-BAC36wt cells (Fig. 3B, lanes 1 and 2). Other lytic transcripts, such as ORFs 25 and K5 and v-IRF2, were also readily detected in both type of cells. Interestingly, appreciable levels of lytic transcripts were also detected in the uninduced cells, which were increased by TPA induction (Fig. 3B). These results suggested the absence of full-length gB expression from the ΔgBBAC36 genome.

Immunoprecipitation reactions confirm the absence of gB in 293T-ΔgBBAC36 cells. To further confirm the absence of gB in ΔgBBAC36, total protein lysates from TPA-induced 293T, 293T-BAC36wt, and 293T-ΔgBBAC36 cells were immunoprecipitated with gB- and gpK8.1A-specific antibodies and tested in Western blot reactions. The KSHV gB ORF is 845 amino acids (aa) long, with a signal sequence (aa 1 to 23) and a transmembrane domain (aa 710 to 729) and with 13 N glycosylation sites. At amino acid positions 440 and 441, there is a potential proteolytic cleavage site (RKRR/S), and cleavage at this site would result in two proteins with the predicted molecular masses of about 48 and 45 kDa (4). In KSHV-carrying BCBL-1 cells, gB is synthesized as a 110-kDa precursor protein and undergoes cleavage and processing, and the envelope-associated gB is made up of 64- and a 54-kDa polypeptides forming disulfide-linked heterodimers and multimers (4). In 293T-BAC36wt cells, the 116-kDa gB precursor and the broadly migrating 64-kDa cleavage products were readily detected (Fig. 3C, lane 1). The 54-kDa polypeptide was not clearly identifiable, as it was probably masked by the heavy chain of anti-gB rabbit antibodies used in the immunoprecipitation reactions. In contrast, these gB proteins were not detected in 293T-ΔgBBAC36 cells (Fig. 3C, lane 2), thus confirming the absence of the gB protein. gpK8.1A was detected in both 293T-BAC36wt and 293T-ΔgBBAC36 cells (Fig. 3C, lanes 4 and 5), demonstrating the specificity of gB deletion. The specificity of these reactions was further confirmed by the absence of KSHV glycoproteins in the control 293T cells (Fig. 3C, lanes 3 and 6).

The full complement of KSHV latent and lytic genes are expressed in stable 293T-BAC36wt and 293T-ΔgBBAC36 cells. When real-time RT-PCR was conducted to detect KSHV viral transcripts, closely similar levels of latency-associated ORF 73 transcript were detected in the uninduced 293T-BAC36wt and 293T-ΔgBBAC36 cells, and a moderate decrease was observed in the TPA-induced cells (Fig. 3D). Closely similar levels of KSHV lytic viral transcripts were also detected in 293T-BAC36wt and 293T-ΔgBBAC36 cells (Fig. 3D). Interestingly, high levels of lytic-cycle ORF 50 (Fig. 3D) and ORF K8 and K5 (data not shown) transcripts (41) were detected in the uninduced cells, which increased in the TPA-induced 293T-BAC36wt and 293T-ΔgBBAC36 cells.

Expression of latency-associated LANA-1 (ORF 73) and lytic ORF 59 proteins was monitored by immunoperoxidase assays to quantitate the cells entering the lytic cycle. ORF 73 proteins were detected in >75% of the uninduced and TPA-induced 293T-BAC36wt and 293T-ΔgBBAC36 cells (Fig. 4A, B, E, and F). About 10 to 15% of uninduced 293T-BAC36wt and 293T-ΔgBBAC36 cells were also expressing the lytic ORF 59 proteins, which increased to >35% after 96 h post-TPA

induction (Fig. 4C, D, G, and H). None of the proteins could be detected in 293T cells, demonstrating the specificity of these reactions. Since 293T cells grew very rapidly, resulting in overcrowding, it was difficult to estimate the percentage of cells expressing these proteins. Nevertheless, these results indicated an active lytic-cycle replication in the uninduced cells and its increase by TPA induction.

Deletion of gB results in the absence of KSHV particles in 293T-ΔgBBAC36 cell supernatant. To determine the effect of gB deletion on infectious-virus formation, 293T-BAC36wt and 293T-ΔgBBAC36 cells were induced with TPA for 96 h and virus was concentrated from the supernatants (38). Viral DNA was pretreated with DNase I or untreated, and equal amounts of DNA were quantitated for KSHV ORF 73 by real-time DNA PCRs. As shown in Fig. 5A, a higher level of virus was detected in BCBL-1 and BAC36wt virus preparations, with about 10^5 to 10^6 viral DNA copy numbers per 100 ng of input DNA. DNase I treatment reduced the virion-associated BCBL-1 and BAC36wt DNA by about 60%. In contrast, only very small amounts of viral DNA could be detected in ΔgB-BAC36 virus preparations, which was about 100 times less than BAC36wt virus, which decreased drastically to undetectable levels after DNase I treatment (Fig. 5A). Similarly, when cells were transfected with ORF 50 regulator of transcription and activation (RTA)-expressing plasmid (5), progeny virus was not observed in 293T-ΔgBBAC36 cells. In contrast, in 293T-BAC36wt, RTA induced virus production, which was comparable to TPA induction (data not shown). The detection of significant quantities of DNase I-susceptible DNA in virus preparations concentrated from the culture supernatants of BCBL-1 cells could be (i) due to the association of virions with viral DNA released from the cells during TPA treatment and cell death and/or (ii) contributed by damaged virions accessible to DNase I treatments. Nevertheless, these results indicated the absence of mature KSHV particles in 293T-ΔgBBAC36 cell supernatants and suggested a defect in the formation or maturation and/or the egress of KSHV as a result of gB deletion.

The infectivities of viruses prepared from BCBL-1, 293T-BAC36wt, and 293T-ΔgBBAC36 cells without DNase I treatment were next tested. HMVEC-d cells were infected with viruses for 2 h at a multiplicity of infection (MOI) of 10 viral DNA copies/cell, and the internalization of virus was tested by real-time DNA PCR. As shown in Fig. 5B, internalization of considerable amounts of BCBL-1 and BAC36wt viral DNA was observed. By this method, we previously observed ~90% infection in the target cells (25). Compared with BAC36wt virus, about 40% increase in internalization was observed with BCBL-KSHV (Fig. 5B). In contrast, no viral DNA internalization was observed with non-DNase I-treated virus preparations from 293T-ΔgBBAC36 cell supernatants (Fig. 5B).

To confirm the infection of HMVEC-d cells with BCBL and BAC36wt-KSHV, cells were infected for 2 h at an MOI of 10 viral DNA copies/cell, and total RNA was isolated, treated with DNase I, and analyzed by real-time RT-PCR to detect viral transcripts. Our studies have shown that in addition to the latent and lytic ORF 50 genes, KSHV also expresses a limited number of lytic-cycle genes early during infection (25). Though some of these viral transcripts detected by gene array in the earlier study could also represent messages carried in the
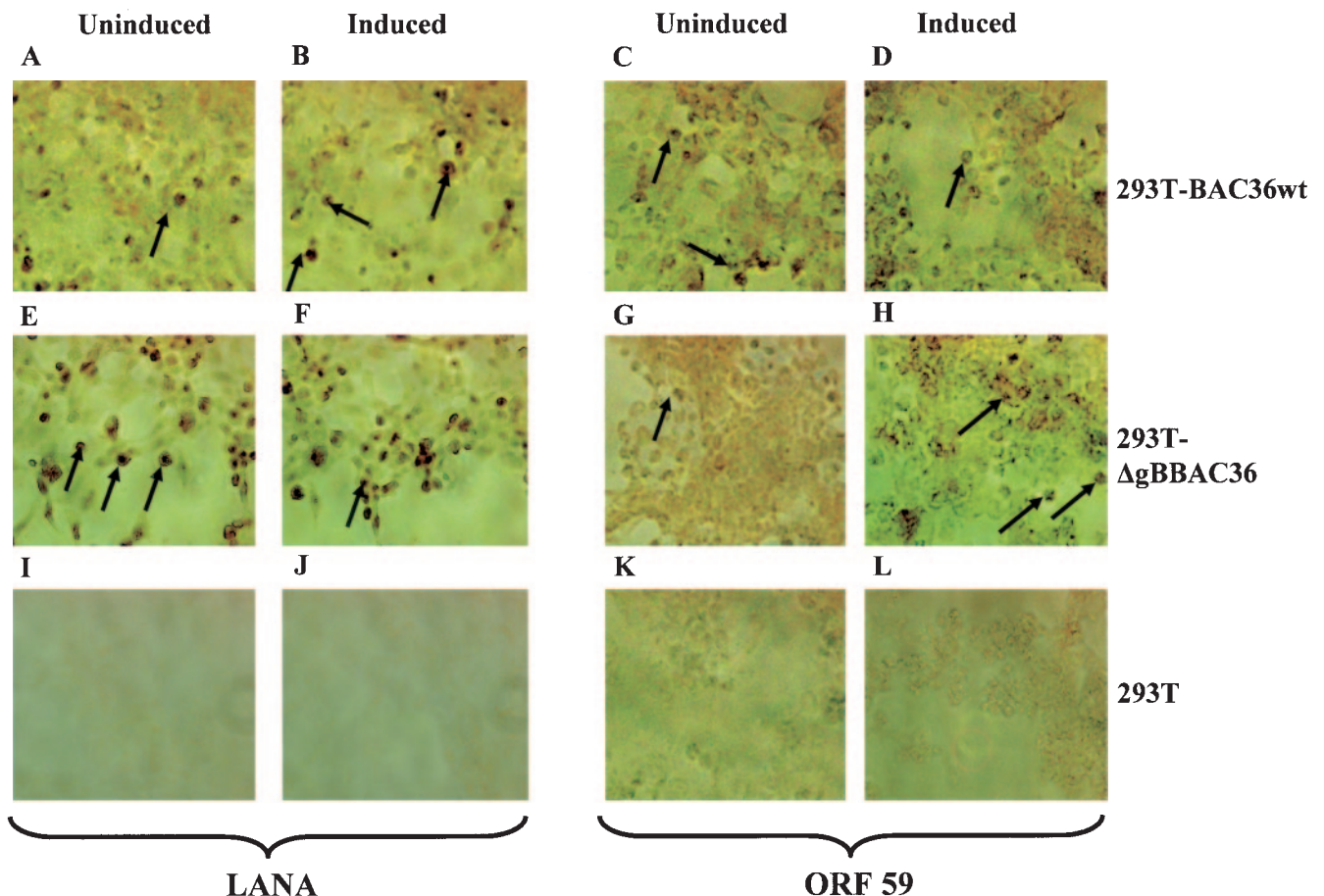
FIG. 4. Immunoperoxidase assay detecting KSHV ORF 73 (LANA) and ORF59 proteins. 293T, 293T-BAC36wt, and 293T-ΔgBBAC36 cells in chamber slides were uninduced (A, C, E, G, I, and K) or induced with 20 ng/ml of TPA for 96 h (B, D, F, H, J, and L), fixed with ice-cold acetone, and treated with 5% hydrogen peroxide to remove endogenous peroxidase. The cells were incubated at room temperature with rabbit anti-ORF 73 antibodies (A, B, E, F, I, and J) or with anti-ORF59 monoclonal antibodies (C, D, G, H, K, and L), washed, and treated with biotinylated secondary antibody followed by ABC reagent. Color reaction was performed with hydrogen peroxide and diaminobenzidine. The arrows indicate the cells stained with the respective antibodies. The total number of cells and the number of cells stained positive by the reaction were counted in at least three separate areas, and the percentage of cells expressing the respective proteins was calculated. Magnification, ×40.

virion particles, further examination revealed a quantitative increase in early lytic K5, K8, and v-IRF2 gene expression in the infected cells (25). As shown in Fig. 5C, the copy numbers of lytic ORF 50 and K8 transcripts and latent ORF 73 transcripts in cells infected with BCBL and BAC36wt-KSHV were closely similar. However, infection with equal or higher DNA copy numbers of ΔgBBAC36 virus failed to initiate any infection. This is not surprising, since no DNase I-resistant viral DNA could be detected in 293T-ΔgBBAC36 cell supernatants. These results suggested that deletion of gB leads to defects in the egress of KSHV.

Electron microscopy reveals the disruption of the KSHV egress pathway by gB deletion. To further evaluate the absence of ΔgBBAC36 virus in the supernatants of 293T-ΔgBBAC36 cells, we next examined the uninduced and TPA-induced cells by electron microscopy. Maturation of herpesviruses is a complex multistep event, and the details of these steps have not been fully deciphered. In the prototypical maturation pathway described for α-herpesviruses, such as herpes simplex virus type 1, PrV, varicella-zoster virus, infectious laryngotrachitis

virus, and equine herpesvirus 1, and for the β-herpesvirus human cytomegalovirus (HCMV), assembly of progeny viral nucleocapsids takes place in the nucleus. These capsids exit the nuclei by budding at the inner nuclear membrane into the perinuclear space, resulting in enveloped particles with a rim of tegument and a smooth envelope surface (33). These enveloped particles egress from the perinuclear space by fusion of the primary envelope with the outer nuclear membrane, a process called deenvelopment. The resulting intracytoplasmic naked nucleocapsids are then reenveloped at *trans*-Golgi network (TGN) membranes, where large amounts of tegument materials are added to the capsids. The reenvelopment step involves the budding of capsid and tegument into the exocytic vesicles inserted with envelope glycoproteins, which is followed by a reverse phagocytic phenomenon involving the fusion of viral-particle-containing vesicles at the plasma membrane, thus releasing the mature enveloped virus particles with condensed core, capsid, and tegument to the extracellular region (33).

Examination of 293T-BAC36wt cells at 96 h post-TPA induction revealed the presence of empty capsids and capsids
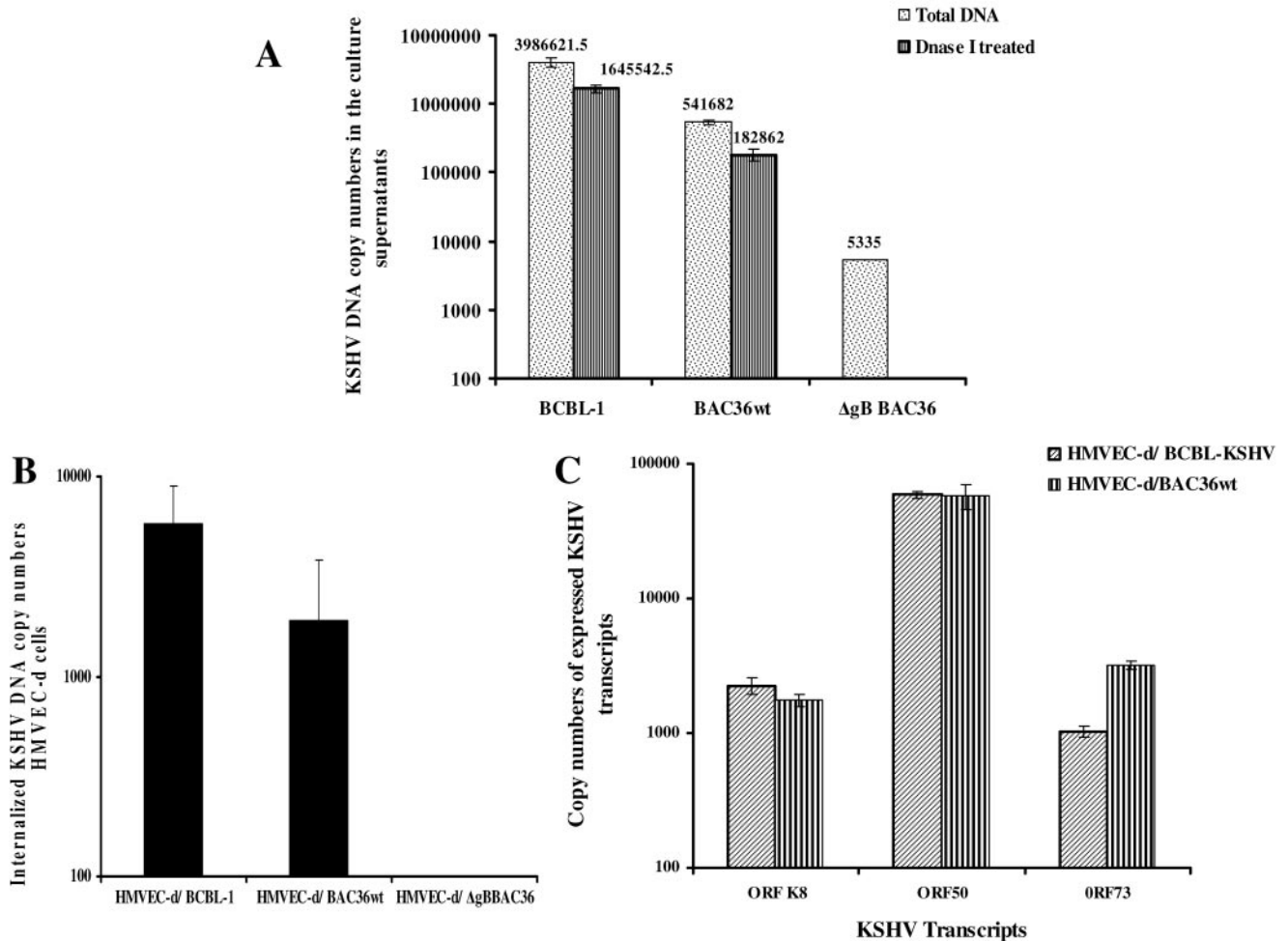
FIG. 5. (A) Egress of BAC36wt and ΔgBBAC36-KSHV. 293T-BAC36wt and 293T-ΔgBBAC cells were induced with 20 ng/ml of TPA for 96 h, and the virus in the supernatants was concentrated (36). Total DNA prepared from the virus stocks was analyzed by real-time DNA PCR to estimate the ORF 73 DNA copy numbers. Virus from TPA-induced BCBL-1 cells was used for comparison. Virus stocks (200 μl) were also pretreated with 12 μg of DNase I for 15 min at room temperature, the reaction was stopped by EDTA followed by heat inactivation at 70°C, and DNA was prepared. The error bars indicate standard deviations. (B) Quantitation of BAC36wt, ΔgBBAC36, and BCBL-KSHV entry into target cells. HMVEC-d cells were infected with KSHV at an MOI of 10 DNA copies per cell for 2 h. After infection, the cells were washed with PBS to remove the unbound virus, treated with trypsin-EDTA for 5 min at 37°C to remove the bound but noninternalized virus, and washed, and then total DNA was isolated. This was normalized, and 100 ng of DNA was used to estimate the KSHV ORF 73 copy numbers by real-time DNA PCR. The threshold cycle values were used to plot the standard graph and to calculate the relative copy numbers of internalized viral DNA in the samples. Each reaction was done in duplicate, and each point represents the average plus the standard deviation of three experiments. (C) Quantitation of copy numbers of expressed KSHV transcripts. HMVEC-d cells were infected with BAC36wt, ΔgBBAC36, and BCBL-KSHV for 2 h, and RNA was collected. Real-time RT-PCRs for ORF 50 and ORF 73 were performed with 250 ng of DNase-treated RNA, and copy numbers were estimated as in the procedures in the legend to Fig. 3D. KSHV transcripts were not detected in cells infected with ΔgBBAC36 virus. The error bars indicate standard deviations.

with condensed cores in the nuclei (Fig. 6A). In the cytoplasm of these cells, capsids with dense cores were detected near the outer membranes of nuclei (Fig. 6B and C), which resembled the deenvelopment stage described for other herpesviruses (9, 23, 20). In addition, vesicles with viral particles with dense cores and envelopes were observed in the *trans*-Golgi region (Fig. 6D and E), which probably represents a reenvelopment stage. Enveloped virus particles enclosing capsids with dark cores (Fig. 6F) were observed in the extracellular region, which indicated successful maturation and egress of the BAC36wt-KSHV.

In contrast, we did not detect any fully enveloped virus

particles in the extracellular compartments of TPA-induced 293T-ΔgBBAC36 cells. Capsids with cores were observed in the nuclei (Fig. 7A). The cytoplasms were filled with numerous vesicles with what appeared to be core-containing capsids in the process of envelopment (Fig. 7B to F and Fig. 8A to D). The cores in the capsid were surrounded by a halo of clear space, and the capsids were surrounded by a large amount of dark particulate fibrous materials probably representing tegument proteins (Fig. 7B to F and Fig. 8A to D). Similarly, large quantities of tegument materials were observed in the reenvelopment stages of infectious laryngotrachitis virus (20). In addition, large vesicles probably representing the exocytic vesi-
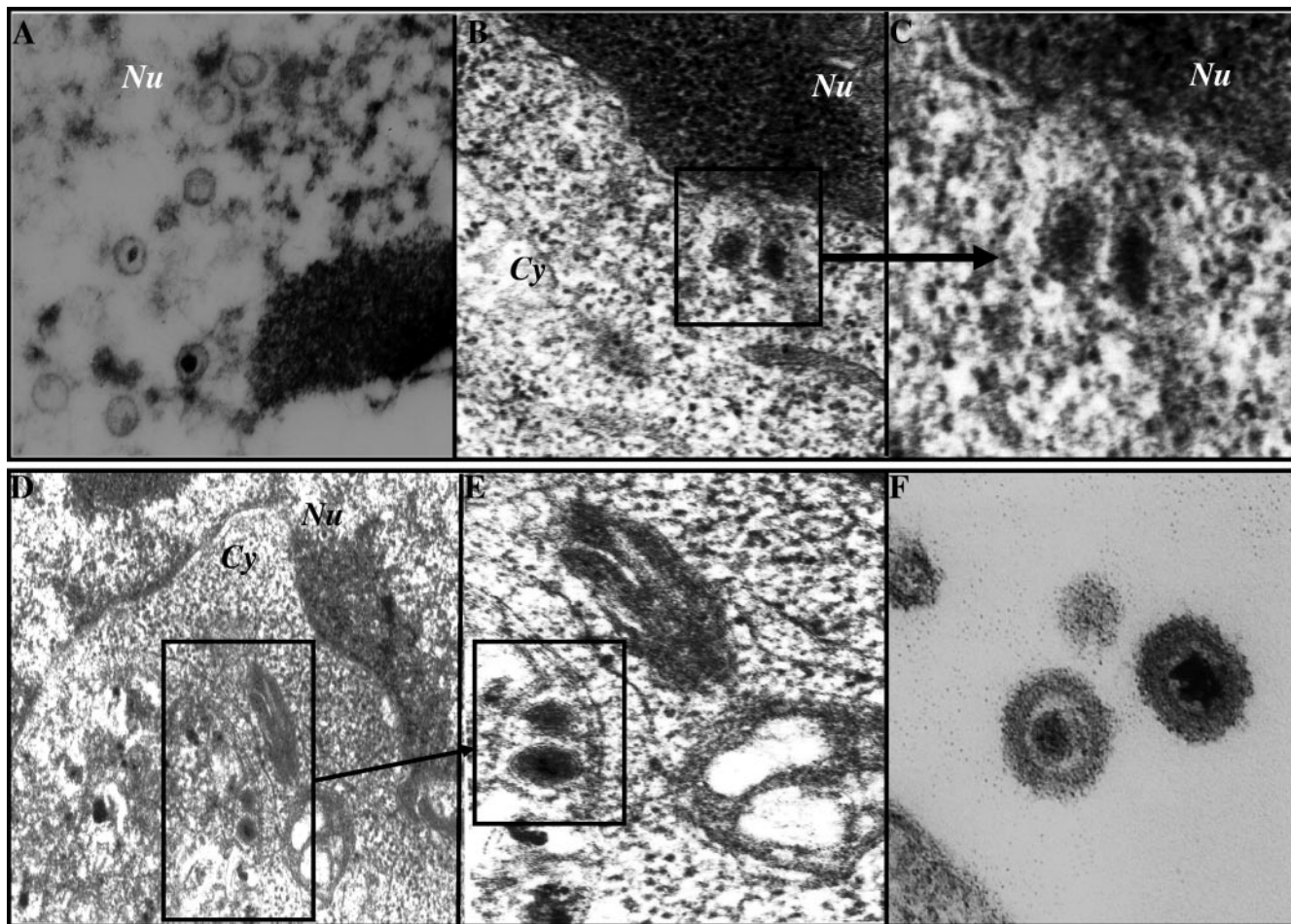
FIG. 6. Electron micrographs of 293T-BAC36wt cells. 293T cells carrying the BAC36wt-KSHV genome were induced with 20 ng/ml of TPA for 96 h, collected, washed in PBS, and fixed in 2% glutaraldehyde. Thin sections were made and observed under a transmission electron microscope (A to F). Panel C is an enlargement of the area in the panel B inset. Panel E is an enlargement of the area in the panel D inset. (F) Extracellular KSHV virus particles. *Nu*, nucleus; *Cy*, cytoplasm. Magnifications: A, ×108,000; B and E, ×87,000; C and F, ×144,000; D, ×57,000.

cles with viral capsid and tegument in the process of budding into the vesicles were observed (Fig. 7D to F and Fig. 8A to D). The envelopment appears to be an incomplete and slow process, and we did not observe condensed core and capsids in the cytoplasm. Occasionally, we observed enveloped virions (Fig. 8E to F). However, unlike BAC36wt-KSHV, the capsids appeared not to be fully condensed around the cores. Together with the absence of extracellular virus particles, this further confirmed that deletion of gB leads to defects in the egress of KSHV.

Complementation of gB restores the ability of ΔgBBAC36-KSHV to egress and infect target cells. To confirm the role of gB in KSHV egress and infection, monolayers of 293T-ΔgBBAC36 cells were transfected with gB-expressing pCDNA3.1 plasmids and induced with TPA after 48 h of transfection, and virus from the supernatant collected after 96 h was analyzed. As seen in Fig. 3C, gB was absent in the 293T-ΔgBBAC36 cells induced with TPA (Fig. 9A, lane 2). Similar to the 293T-BAC36wt cells (Fig. 9A, lane 1), glycosylated polypeptides of gB were readily detected in the ΔgBBAC36 cells transfected with gB-expressing pCDNA3.1, while they

could not be detected in the ΔgBBAC36 cells transfected with pCDNA3.1 plasmid alone, confirming the exogenous expression of gB from the plasmid (Fig. 9A, lanes 3 and 4, respectively). As shown in Fig. 9B, transfection of gB restored the DNase I-resistant virus production in the supernatants of 293T-ΔgBBAC36 cells. The gB-complemented ΔgBBAC36 viruses were used to infect HMVEC-d cells, and real-time RT-PCR results showed that complemented ΔgBBAC36 viruses entered the target cells and expressed the ORF 73 transcripts with efficiency similar to that of BAC36wt-KSHV (Fig. 9C). These results demonstrated that the viruses recovered from 293T-ΔgBBAC36 cells transfected with gB plasmid could complement the loss of gB in the genome, leading to the maturation and egress of infectious virions.

To further confirm the above findings, viral particles in the concentrated supernatants were examined under an electron microscope after being stained with uranyl acetate (Fig. 10). Enveloped viral particles were seen in the supernatant collected from BCBL-1 and 293T-BAC36wt cells (Fig. 10A and B). However, no intact enveloped virions were observed in the supernatant concentrated from 293T-ΔgBBAC36 cells, and instead, par-
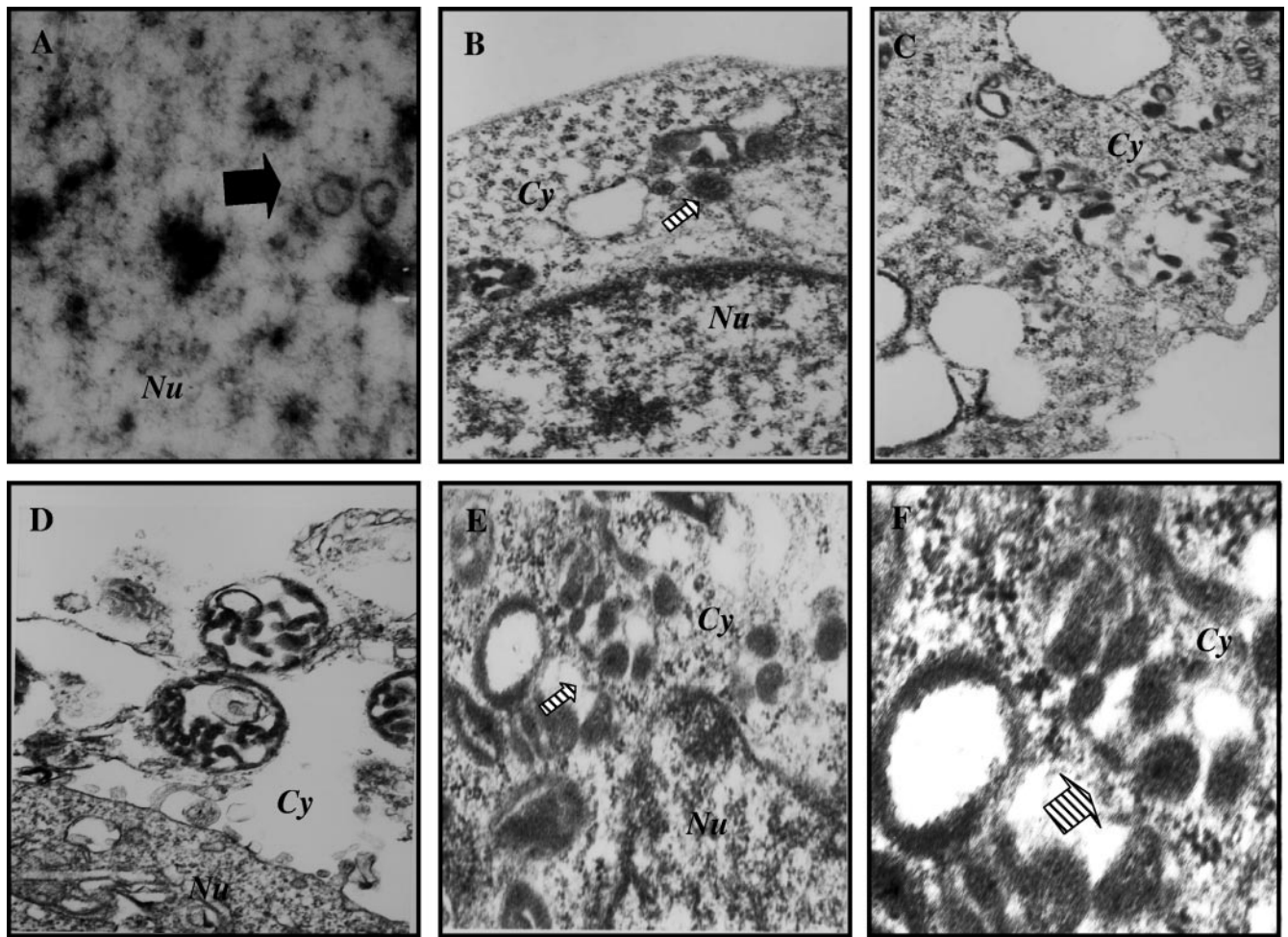
FIG. 7. Electron micrographs of 293T-ΔgBBAC36 cells. 293T cells carrying the ΔgB BAC36-KSHV genome were induced with 20 ng/ml of TPA for 96 h, collected, washed in PBS, and fixed in 2% glutaraldehyde. The bold arrow in panel A indicates the capsids in the nucleus. The striped white arrows in panels B, E, and F indicate vesicles in the cytoplasm with core-containing capsids in the process of envelopment. Panel F is an enlargement of areas in panel E demonstrating the core-containing capsids in the process of envelopment. *Nu*, nucleus; *Cy*, cytoplasm. Magnifications: A, ×108,000; B, C, D, and E, ×57,000; F, ×144,000.

ticles resembling capsids with cores clustered together with cellular debris were observed (Fig. 10C). Individual virus particles could not be detected in the supernatants, confirming that egress was affected in these cells. In contrast, intact enveloped virions were readily detected in the supernatants of 293T-ΔgBBAC36 cells transfected with gB-pCDNA3.1 plasmids (Fig. 10D), confirming the successful complementation of egress by exogenously expressed gB. These experiments clearly demonstrated that gB is important for KSHV egress and that deletion of gB in KSHV results in a defect in egress in 293T cells, leading to the nonproduction of mature virus in the supernatant.

DISCUSSION

Envelope glycoproteins of herpesviruses play important roles, not only in virus binding and entry into the target cells, but also in the assembly, maturation, migration, and release of progeny virus particles from the infected cells. Like other herpesviruses, KSHV encodes several envelope glycoproteins, and previous studies demonstrating the interaction of KSHV-gB with cell surface heparan sulfate and α3β1 integrin molecules and the subsequent stimulation of host cell signaling (3, 6, 58) have shown the importance of gB in KSHV infection of target cells. In the present study, we demonstrate that besides its role in virus binding and entry, KSHV gB also plays a significant role in virus egress.

To monitor the maintenance of KSHV genomes in 293T cells developed for these studies, we checked the expression of GFP from the BAC clone during successive passages of these cells. GFP was expressed in all the cells, and we also detected LANA-1 protein by immunoperoxidase assay in ~75% of the cells. Lytic-cycle ORF 59 protein was detected in ~10 to 15% of uninduced cells and in ~35% of cells after induction with TPA. Even though eGFP was expressed in all of the stably transfected cells, we also observed higher fluorescence intensity in ~10% of uninduced cells. These could represent cells spontaneously entering the lytic cycle, since we observed higher levels of lytic-cycle transcripts in TPA-induced 293T-BAC36wt and 293T-ΔgBBAC36 cells than in uninduced BCBL-1 cells. The copy numbers of BAC36wt-KSHV collected
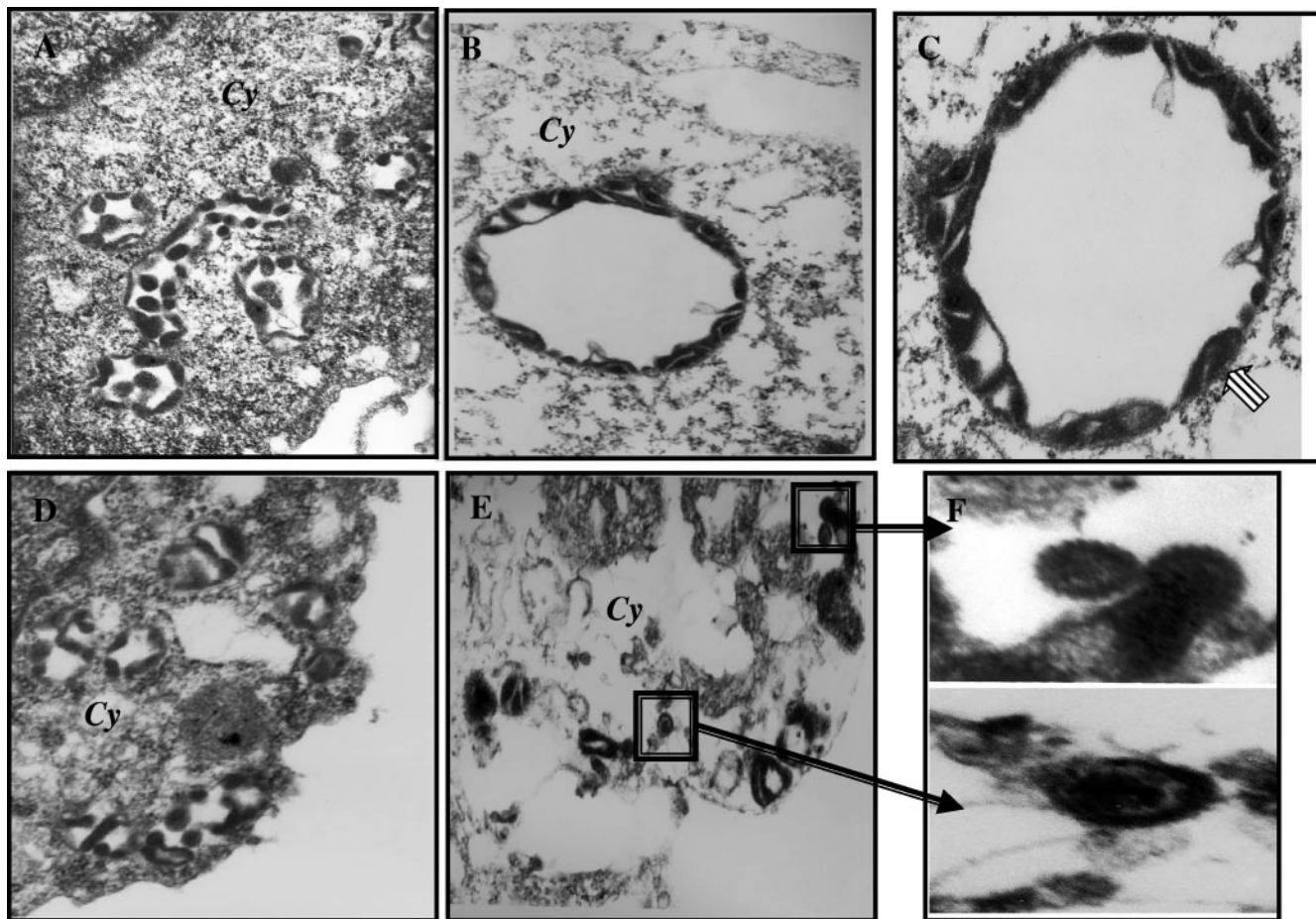
FIG. 8. Electron micrographs of 293T-ΔgBBAC36 cells. 293T cells carrying the ΔgBBAC36-KSHV genome were induced with 20 ng/ml of TPA for 96 h, collected, washed in PBS, and fixed in 2% glutaraldehyde. The striped white arrow in panel C indicates vesicles in the cytoplasm with core-containing capsids in the process of envelopment. Panels F and G are enlargements of the areas in the panel E insets demonstrating the occasional enveloped virions with capsids that appeared not to be fully condensed around the cores. *Nu*, nucleus; *Cy*, cytoplasm. Magnifications: A, ×108,000; B, D, and E, ×57,000; C and F, ×144,000.

from TPA-induced monolayer cells from fifteen 75-cm^2 flasks were about 5 to 10 times less than that of KSHV collected from 900 ml of TPA-induced BCBL-1 culture. This could be due to a smaller number of viral genomes in 293T cells than in BCBL-1 cells, which are reported to carry about 80 copies of viral genomes. The number of BAC36 genome copies in 293T cells was not determined.

DNase I-resistant viral DNA and infectious virus in the supernatants of 293T-ΔgBBAC36 cells induced with either TPA or KSHV RTA could not be detected. Even though we could not use the biologically relevant human primary endothelial (HMVEC-d) cells due to poor transfection efficiency and selection, detection of infectious virus in the supernatants of 293T-BAC36wt cells clearly demonstrated the ability of 293T cells to support the normal egress process of wild-type KSHV. Introduction of gB-pCDNA3.1 plasmids into 293T-ΔgBBAC36 cells resulted in the detection of DNase I-resistant virus in the supernatant, which was about 40% of the BAC36wt virus particles detected from the 293T-BAC36wt cells. Even though pCDNA3.1 plasmids could be transfected with ~90% efficiency, the lower percentage of virus detection could be due

to a possible stoichiometric effect of the ectopically expressed gB molecules in the formation of mature virions. However, the ability of KSHV from 293T-ΔgBBAC36 cells after complementation to infect HMVEC-d cells with efficiency similar to that of BAC36wt virus confirmed the role of gB in the egress process.

Conservation of envelope glycoprotein gB among the members of the herpesvirus family indicates the functional importance of gB in the viral replicative cycle (53, 54). While studies have demonstrated the role of gB in the binding and entry processes of different herpesviruses, its role in the egress process appears to vary according to the virus system examined. For example, PrV gB was first shown to be required for egress and in the absence of complementation; infection of swine kidney cells (SK-6) by PrV-gB mutant virus led to the accumulation of enveloped viral particles between the inner and outer nuclear membranes (43). However, a later contradictory study showed that gB is not required in this process (20). In contrast, and similar to our studies, the gamma 1-EBV gB (gp110) has been shown to play an important role in virus assembly and egress (29, 34). Analogous to the 293T-ΔgB-
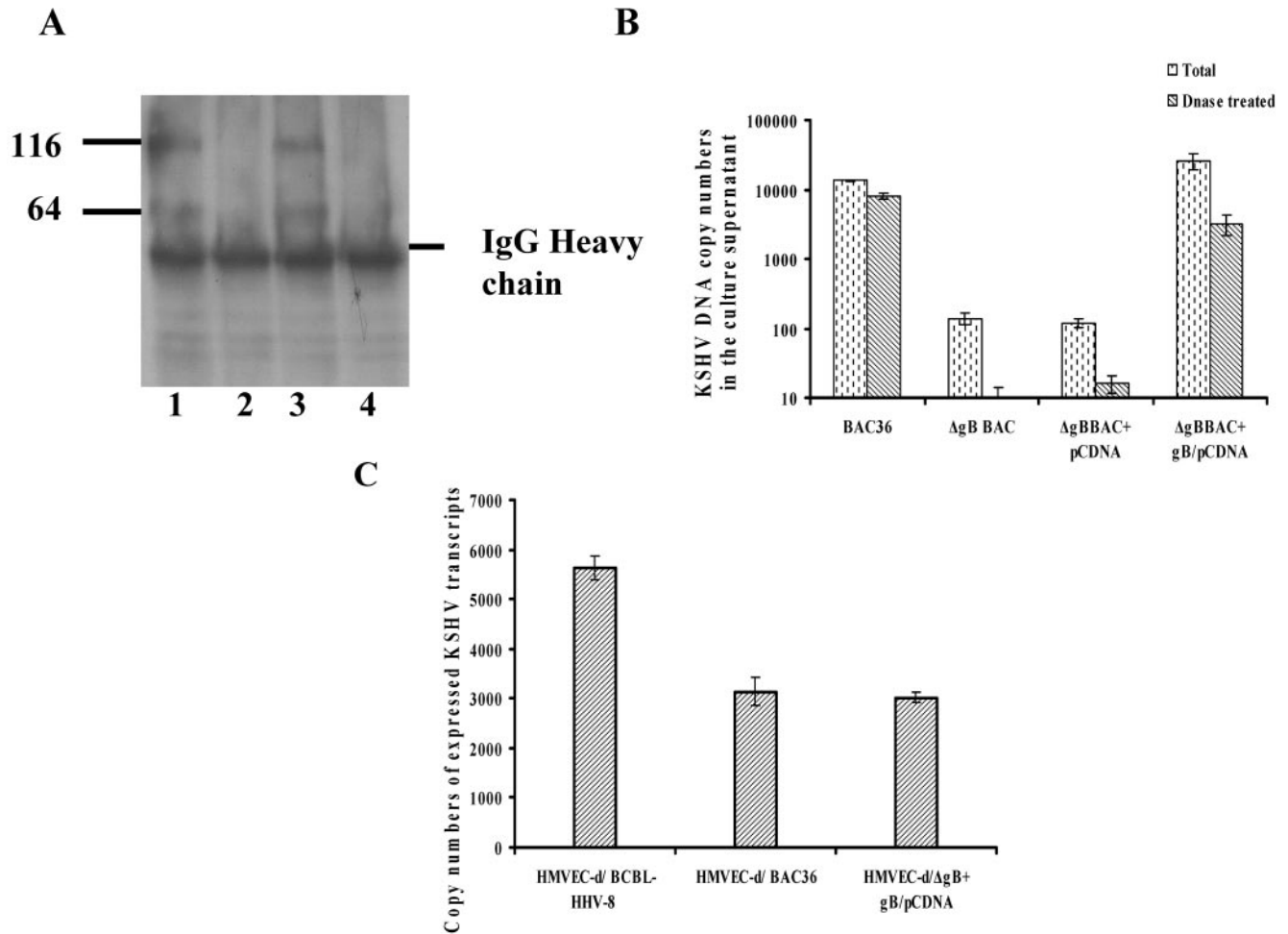
FIG. 9. Complementation of ΔgBBAC with gB. (A) Monolayers of 293T-ΔgBBAC36 cells were transfected with gB-pCDNA3.1 plasmid or pCDNA3.1 plasmid for 48 h and induced with TPA for 96 h, and lysates were prepared in RIPA lysis buffer. KSHV gB was immunoprecipitated with rabbit anti-gB polyclonal antibodies, Western blotted, reacted with anti-gB antibodies, and tested with alkaline phosphatase-conjugated secondary antibodies (lanes 3 and 4). Lysates from untransfected 293T-BAC36wt and 293T-ΔgBBAC36 cells induced with TPA for 96 h were also immunoprecipitated and Western blotted (lanes 1 and 2). The numbers indicate the molecular masses (in kilodaltons) of the gB proteins detected. (B) Monolayers of 293T-ΔgBBAC36 cells transfected with gB-pCDNA3.1 plasmid or pCDNA3.1 plasmid alone as the control for 48 h and induced with TPA for 96 h. KSHV was concentrated from the culture supernatants, and total DNA was isolated and subjected to real-time DNA PCR to quantitate the ORF 73 copy numbers. Virus stocks were also pretreated with 12 μg of DNase I for 15 min at room temperature. (C) HMVEC-d cells were infected with virus from 293T-ΔgBBAC36 cells complemented with gB-pCDNA3.1 plasmid, and copy numbers of expressed KSHV transcripts were quantitated as in the procedures described in the legend to Fig. 3D. The error bars indicate standard deviations.

BAC36 cells reported in the present study, no enveloped EBV particles were observed in TPA-induced lymphoblastoid cell lines carrying a Δgp110 EBV genome (29). Based on these studies, the authors concluded that EBVgB may provide signals necessary for the assembly of EBV nucleocapsids and their egress from the nuclei of the infected cells and that EBVgB may have evolved functions different from those of gB homologs of α-herpesviruses (29).

The absence of DNase I-resistant viral DNA, as well as enveloped virus particles, in the supernatant of 293T-ΔgB-BAC36 cells, together with the recovery of infectious KSHV after complementation, clearly demonstrated the important role of gB in the maturation and egress of infectious gamma 2 KSHV. The stages of maturation and egress that require KSHV gB and the mechanism are not known at present and

need to be investigated. Compared to 293T-BAC36wt cells, vesicles filled with virus particles possibly representing the re-envelopment stage in the cytoplasm were more readily observed in the 293T-ΔgBBAC36 cells. Since several tegument proteins of herpesviruses are believed to interact with envelope glycoproteins during the reenvelopment stages (33), easy detection of these vesicles could represent an inefficient and slow envelopment process due to the absence of gB. This suggests that gB must play an important role in the envelopment stage (60). This envelopment process is believed to occur by the budding of capsid and tegument into the late secretory pathway organelle, the TGN, and/or the associated endosomal compartment (33). HCMV gB has been shown to interact with the phosphofurin acidic cluster sorting protein 1 (PACS-1), a connector protein that is required for the trafficking of proteins

BCBL-1 KSHV

Bac36 wt-KSHV

ΔgBBAC36-KSHV

ΔgBBAC36-KSHV+gB-pCDNA
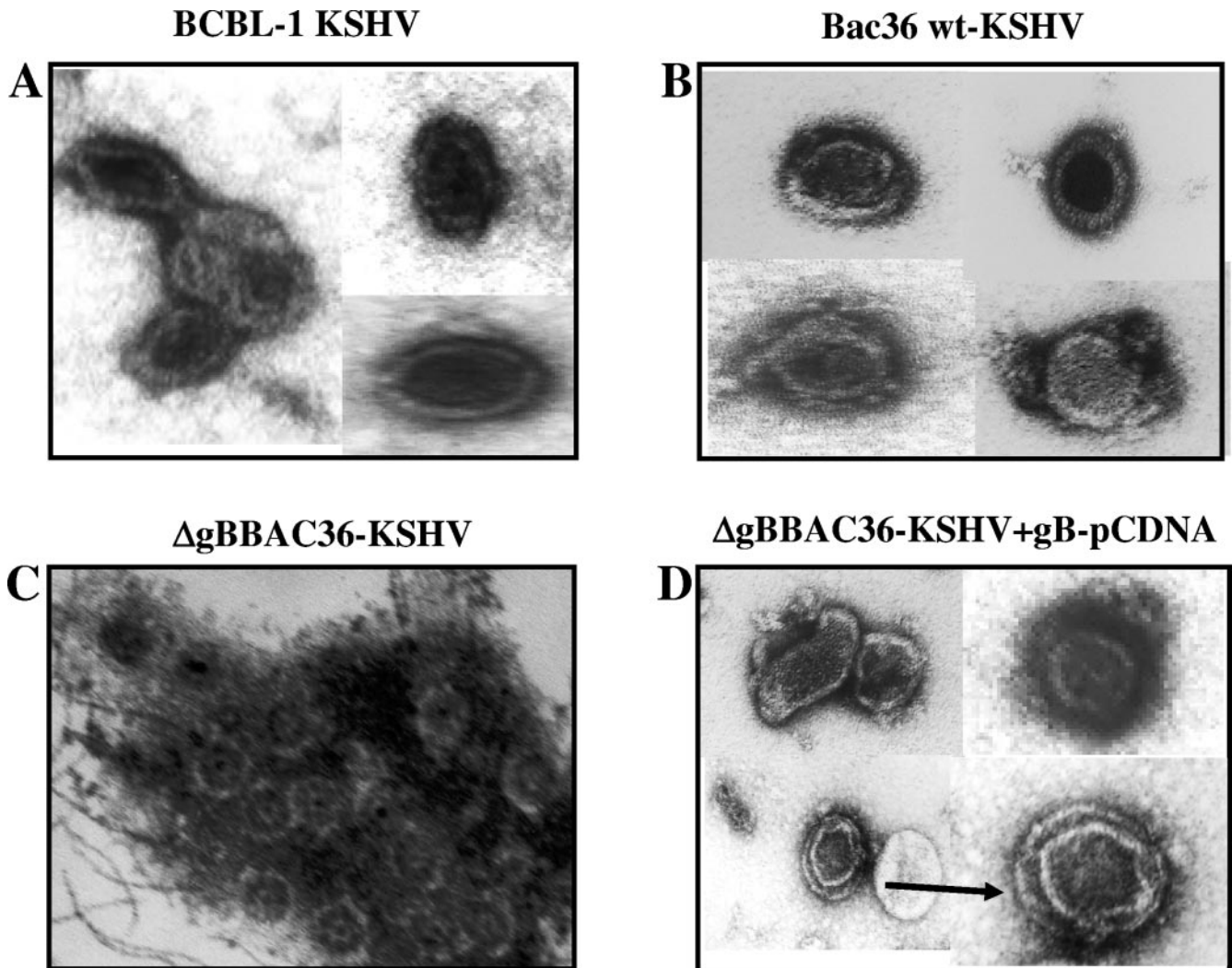
FIG. 10. Electron micrographs of virus particles. Virus particles in the supernatants of TPA-induced BCBL-1 cells (A), 293T-BAC36 wt cells (B), 293T-ΔgBBAC36 cells (C), and 293T-ΔgBBAC36 cells transfected with gB-pCDNA3.1 plasmid (D) were concentrated, stained with 1% uranyl acetate in distilled water for 30 s, and observed under an electron microscope. Magnifications, ×144,000.

(14). PACS-1 was required for the correct localization of HCMV gB to the TGN but not for HCMV gH localization. Inhibition of PACS-1 activity led to a decrease in the HCMV titer, and an increase in expression of PACS-1 increased the HCMV titer. These results suggested that HCMV gB interaction with PACS-1 is essential for the efficient production of HCMV, presumably in envelopment and intracellular trafficking. It is possible that KSHV gB may also be interacting with tegument and host proteins and that it plays a role similar to that of HCMV gB in the virus maturation pathway. Envelope glycoproteins of herpesviruses are believed to be essential for the fusion of exocytic vesicles with the plasma membrane and thus the release of enveloped virus particles to the extracellular compartments (33). The absence of DNase I-resistant viral DNA and enveloped virus particles in the 293T-ΔgBBAC36 cell supernatants and the presence of occasional enveloped particles in the cytoplasm suggest that KSHV gB may also have a role in the release of enveloped virus particles.

In summary, our studies suggest that KSHV gB plays significant roles in virus binding, entry, and egress, and further studies are under way to decipher the role of KSHV gB in the different stages of envelopment and maturation of infectious virus particles.

REFERENCES

1. **Akula, S. M., P. P. Naranatt, N. S. Walia, F. Z. Wang, B. Fegley, and B. Chandran.** 2003. Kaposi's sarcoma-associated herpesvirus (human herpesvirus 8) infection of human fibroblast cells occurs through endocytosis. J. Virol. **77:**7978–7990.
2. **Akula, S. M., N. P. Pramod, F.-Z. Wang, and B. Chandran.** 2002. Integrin α3β1 (CD49c/28) is a cellular receptor for Kaposi's sarcoma associated herpesvirus (KSHV/HHV-8) entry into the target cells. Cell **108:**407–419.
3. **Akula, S. M., F.-Z. Wang, J. Vieira, and B. Chandran.** 2001. Human her-

pesvirus 8 interaction with target cells involves heparan sulfate. Virology **282:**245–255.

4. **Akula, S. M., N. P. Pramod, F. Z. Wang, and B. Chandran.** 2001. Human herpesvirus envelope-associated glycoprotein B interacts with heparan sulfate-like moieties. Virology **284:**235–249.

4a.**Ausubel, R., R. Brent, R. Kingston, D. Moore, J. A. Smith, J. Seidman, and K. Struhl (ed.).** 1989. Current protocols in molecular biology, vol. 1. John Wiley & Sons, New York, N.Y.

5. **Bechtel, J. T., Y. Liang, J. Hvidding, and D. Ganem.** 2003. Host range of Kaposi's sarcoma-associated herpesvirus in cultured cells. J. Virol. **77:**6474–6481.

6. **Birkmann, A., A. Mahr, A. Ensser, S. Yaguboglu, F. Titgemeyer, B. Fleckenstein, and F. Neipel.** 2001. Cell surface heparan sulfate is a receptor for human herpesvirus 8 and interacts with envelope glycoprotein K8.1. J. Virol. **75:**11583–11593.

7. **Blackbourn, D. J., E. Lennette, B. Klencke, A. Moses, B. Chandran, M. Weinstein, R. G. Glogau, M. H. Witte, D. L. Way, T. Kutzkey, B. Herndier, and J. A. Levy.** 2000. The restricted cellular host range of human herpesvirus 8. AIDS **14:**1123–1133.

8. **Boshoff, C., T. F. Schulz, M. M. Kennedy, A. K. Graham, C. Fisher, A. Thomas, J. O. McGee, R. A. Weiss, and J. J. O'Leary.** 1995. Kaposi's sarcoma-associated herpesvirus infects endothelial and spindle cells. Nat. Med. **1:**1274–1278.

9. **Brack, A. R., J. Dijkstra, H. Granzow, B. G. Klupp, and T. C. Mettenleiter.** 1999. Inhibition of virion maturation by simultaneous deletion of glycoproteins E, I, and M of pseudorabies virus. J. Virol. **73:**5364–5372.

10. **Cesarman, E., Y. Chang, P. S. Moore, J. W. Said, and D. M. Knowles.** 1995. Kaposi's sarcoma-associated herpesvirus-like DNA sequences are present in AIDS-related body cavity based lymphomas. N. Engl. J. Med. **332:**1186–1191.

11. **Chan, S. R., C. Bloomer, and B. Chandran.** 1998. Identification and characterization of human herpesvirus-8 lytic cycle associated ORF 59 protein and the encoding cDNA by monoclonal antibody. Virology **240:**118–128.

12. **Chandran, B., S. Bloomer, S. R. Chan, L. Zhu, E. Goldstein, and R. Horvat.** 1998. Human herpesvirus-8 ORF K8.1 gene encodes immunogenic glycoproteins generated by spliced transcripts. Virology **249:**140–149.

13. **Chang, Y., E. Cesarman, M. S. Pessin, F. Lee, J. Culpepper, D. M. Knowles, and P. S. Moore.** 1994. Identification of herpesvirus-like DNA sequences in AIDS-associated Kaposi's sarcoma. Science **266:**1865–1869.

14. **Crump, C. M., C.-H. Hung, L. Thomas, L. Wan, and G. Thomas.** 2003. Role of PACS-1 in the trafficking of human cytomegalovirus glycoprotein B and virus production. J. Virol. **77:**11105–11113.

15. **Dezube, B. J., M. Zambela, D. R. Sage, J.-F. Wang, and J. D. Fingeroth.** 2002. Characterization of Kaposi sarcoma-associated herpesvirus/human herpesvirus-8 infection of human vascular endothelial cells: early events. Blood **100:**888–896.

16. **Dourmishev, L. A., A. L. Dourmishev, D. Palmeri, R. A. Schwartz, and D. M. Lukac.** 2003. Molecular genetics of Kaposi's sarcoma-associated herpesvirus (human herpesvirus-8) epidemiology and pathogenesis. Microbiol. Mol. Biol. Rev. **67:**175–212.

17. **Ganem, D.** 1997. KSHV and Kaposi's sarcoma: the end of the beginning? Cell **91:**157–160.

18. **Gao, S. J., J. H. Deng, and F. C. Zhou.** 2003. Productive lytic replication of a recombinant Kaposi's sarcoma-associated herpesvirus in efficient primary infection of primary human endothelial cells. J. Virol. **77:**9738–9749.

19. **Giancotti, F. G., and E. Ruoslahti.** 1999. Integrin signaling. Science **285:**1028–1032.

20. **Granzow, H., B. G. Klupp, W. Fuchs, J. Veits, N. Osterrieder, and T. C. Mettenleiter.** 2001. Egress of alphaherpesviruses: comparative ultrastructural study. J. Virol. **75:**3675–3684.

21. **Grundhoff, A., and D. Ganem.** 2004. Inefficient establishment of KSHV latency suggests an additional role for continued lytic replication in Kaposi sarcoma pathogenesis. J. Clin. Investig. **113:**124–136.

22. **Inoue, N., J. Winter, R. B. Lal, M. K. Offermann, and S. Koyano.** 2003. Characterization of entry mechanisms of human herpesvirus 8 by using an Rta-dependent reporter cell line. J. Virol. **77:**8147–8152.

23. **Klupp, B. G., H. Granzow, E. Mundt, and T. C. Mettenleiter.** 2001. Pseudorabies virus UL37 gene product is involved in secondary envelopment. J. Virol. **75:**8927–8936.

24. **Koyano, S., E. C. Mar, F. R. Stamey, and N. Inoue.** 2003. Glycoproteins M and N of human herpesvirus 8 form a complex and inhibit cell fusion. J. Gen. Virol. **84:**1485–1491.

25. **Krishnan, H. H., P. P. Naranatt, M. S. Smith, L. Zeng, C. Bloomer, and B. Chandran.** 2004. Concurrent expression of latent and a limited number of lytic genes with immune modulation and antiapoptotic function by Kaposi's sarcoma-associated herpesvirus early during infection of primary endothelial and fibroblast cells and subsequent decline of lytic gene expression. J. Virol. **78:**3601–3620.

26. **Lagunoff, M., J. Bechtel, E. Venetsanakos, A. M. Roy, N. Abbey, B. Herndier, M. McMahon, and D. Ganem.** 2002. De novo infection and serial transmission of Kaposi's sarcoma-associated herpesvirus in cultured endothelial cells. J. Virol. **76:**2440–2448.

27. **Lake, C. M., and L. M. Hutt-Fletcher.** 2000. Epstein-Barr virus that lacks glycoprotein gN is impaired in assembly and infection. J. Virol. **74:**11162–11172.

28. **Le Doux, J. M., N. Landazuri, M. L. Yarmunsh, and J. R. Morgan.** 2001. Complexation of retrovirus with cationic and anionic polymers increases the efficiency of gene transfer. Hum. Gene Ther. **12:**1611–1621.

29. **Lee, S. K., and R. Longnecker.** 1997. The Epstein-Barr virus glycoprotein 110 carboxy-terminal tail domain is essential for lytic virus replication. J. Virol. **71:**4092–4097.

30. **Li, E., D. Stupack, R. Klemke, D. A. Cheresh, and G. R. Nemerow.** 1998. Adenovirus endocytosis via α_v integrins requires phosphoinositide-3-OH kinase. J. Virol. **72:**2055–2061.

31. **Luna, R. E., F. Zhou, A. Baghian, V. Chouljenko, B. Forghani, S. J. Gao, and K. G. Kousoulas.** 2004. Kaposi's sarcoma-associated herpesvirus glycoprotein K8.1 is dispensable for virus entry. J. Virol. **78:**6389–6398.

32. **McLean, G. W., V. J. Fincham, and M. C. Frame.** 2000. V-Src induces tyrosine phosphorylation of focal adhesion kinase independently of tyrosine 397 and formation of a complex with Src. J. Biol. Chem. **275:**23333–23339.

33. **Mettenleiter, T. C.** 2002. Herpesvirus assembly and egress. J. Virol. **76:**1537–1547.

34. **Miller, N., and L. M. Hutt-Fletcher.** 1992. Epstein-Barr virus enters B cells and epithelial cells by different routes. J. Virol. **66:**3409–3414.

35. **Moore, P. S., and Y. Chang.** 2002. Kaposi's sarcoma associated herpesvirus, p. 2803–2833. *In* D. M. Knipe and P. M. Howley (ed.), Fields virology. Lippincott Williams and Wilkins, Philadelphia, Pa.

36. **Moses, A. V., K. N. Fish, R. Ruhl, P. P. Smith, J. G. Strussenberg, L. Zhu, B. Chandran, and J. A. Nelson.** 1999. Long-term infection and transformation of dermal microvascular endothelial cells by human herpesvirus 8. J. Virol. **73:**6892–6902.

37. **Naranatt, P. P., S. M. Akula, and B. Chandran.** 2002. Characterization of γ2-human herpesvirus-8 glycoproteins gH and gL. Arch. Virol. **147:**1349–1370.

38. **Naranatt, P. P., S. M. Akula, C. A. Zien, H. H. Krishnan, and B. Chandran.** 2003. Kaposi's sarcoma-associated herpesvirus induces phosphatidylinositol 3-kinase-PKC-ζ-MEK-ERK signaling pathway in target cells early during infection: implications for infectivity. J. Virol. **77:**1524–1539.

39. **Narayanan, K., R. Williamson, Y. Zhang, A. F. Stewart, and P. A. Ioannou.** 1999. Efficient and precise engineering of a 200 kb beta-globin human/bacterial artificial chromosome in *E. coli* DH10B using an inducible homologous recombination system. Gene Ther. **6:**442–447.

40. **Neipel, F., J. C. Albrecht, and B. Fleckenstein.** 1997. Cell-homologous genes in the Kaposi's sarcoma-associated rhadinovirus human herpesvirus 8: determinants of its pathogenicity? J. Virol. **71:**4187–4192.

41. **Okuno, T., Y. B. Jiang, K. Ueda, K. Nishimura, T. Tamura, and K. Yamanishi.** 2002. Activation of human herpesvirus 8 open reading frame K5 independent of ORF50 expression. Virus Res. **90:**77–89.

42. **Orford, M., M. Nefedov, J. Vadolas, F. Zaibak, R. Williamson, and P. A. Ioannou.** 2000. Engineering EGFP reporter constructs into a 200 kb human beta-globin BAC clone using GET recombination. Nucleic Acids Res. **28:**E84.

43. **Peeters, B., N. de Wind, M. Hooisma, F. Wagenaar, A. Gielkens, and R. Moormann.** 1992. Pseudorabies virus envelope glycoproteins gp50 and gII are essential for virus penetration, but only gII is involved in membrane fusion. J. Virol. **66:**894–905.

44. **Pereira, L.** 1994. Function of glycoprotein B homologues of the family Herpesviridae. Infect. Agents Dis. **3:**9–28.

45. **Renne, R., W. Zhong, B. Herndier, M. McGrath, N. Abbey, D. Kedes, and D. Ganem.** 1996. Lytic growth of Kaposi's sarcoma-associated herpesvirus (human herpesvirus 8) in culture. Nat. Med. **2:**342–346.

46. **Renne, R., D. Blackbourn, D. Whitby, J. Levy, and D. Ganem.** 1998. Limited transmission of Kaposi's sarcoma-associated herpesvirus in cultured cells. J. Virol. **72:**5182–5188.

47. **Russo, J. J., R. A. Bohenzky, M. C. Chien, J. Chen, M. Yan, D. Maddalena, J. P. Parry, D. Peruzzi, I. S. Edelman, Y. Chang, and P. S. Moore.** 1996. Nucleotide sequence of the Kaposi sarcoma-associated herpesvirus (HHV8). Proc. Natl. Acad. Sci. USA **93:**14862–14867.

48. **Schulz, T. F., Y. Chang, and P. S. Moore.** 1998. Kaposi's sarcoma associated herpesvirus (human herpesvirus 8), p. 87–134. *In* D. J. McCance (ed.), Human tumor viruses. American Society for Microbiology, Washington, D.C.

49. **Schulz, T. F., J. Sheldon, and J. Greensill.** 2002. Kaposi's sarcoma associated herpesvirus (KSHV) or human herpesvirus 8 (HHV-8). Virus Res. **82:**115–126.

50. **Sharma-Walia, N., P. P. Naranatt, H. H. Krishnan, L. Zeng, and B. Chandran.** 2004. Kaposi's sarcoma-associated herpesvirus/human herpesvirus 8 envelope glycoprotein gB induces the integrin-dependent focal adhesion kinase–Src–phosphatidylinositol 3-kinase–rho GTPase signal pathways and cytoskeletal rearrangements. J. Virol. **78:**4207–4223.

51. **Sharma-Walia, N., H. H. Krishnan, P. P. Naranatt, L. Zeng, M. S. Smith, and B. Chandran.** 2005. ERK1/2 and MEK1/2 induced by Kaposi's sarcoma associated herpesvirus (human herpesvirus 8) early during infection of target

cells are essential for expression of viral genes and for establishment of infection. J. Virol **79:**10308–10329.

52. **Soulier, J., L. Grollet, E. Oksenhendler, P. Cacoub, D. Cazals-Hatem, M. F. Babinet, P. d'Agay, J. P. Clauvel, M. Raphael, and L. Degos.** 1995. Kaposi's sarcoma-associated herpesvirus-like DNA sequences in multicentric Castleman's disease. Blood **86:**1276–1280.

53. **Spear, P. G.** 1993. Membrane fusion induced by herpes simplex virus, p. 201–232. *In* J. Bentz (ed.), Viral fusion mechanisms. CRC Press Inc., Ann. Arbor, Mich.

54. **Spear, P. G., and R. Longnecker.** 2003. Herpesvirus entry: an update. J. Virol. **77:**10179–10185.

55. **Staskus, K. A., W. Zhong, K. Gebhard, B. Herndier, H. Wang, R. Renne, J. Beneke, J. Pudney, D. J. Anderson, D. Ganem, and A. T. Haase.** 1997. Kaposi's sarcoma-associated herpesvirus gene expression in endothelial (spindle) tumor cells. J. Virol. **71:**715–719.

56. **Tomescu, C., W. K. Law, and D. H. Kedes.** 2003. Surface down regulation of major histocompatibility complex class I, PE-CAM, and ICAM-1 following de novo infection of endothelial cells with Kaposi's sarcoma-associated herpesvirus. J. Virol. **77:**9669–9684.

57. **Vieira, J., P. O'Hearn, L. Kimball, B. Chandran, and L. Corey.** 2001. Activation of Kaposi's sarcoma-associated herpesvirus (human herpes-virus 8) lytic replication by human cytomegalovirus. J. Virol. **75:**1378–1386.

58. **Wang, F.-Z., S. M. Akula, N. P. Pramod, L. Zeng, and B. Chandran.** 2001. Human herpesvirus 8 envelope glycoprotein K8.1A interaction with the target cells involves heparan sulfate. J. Virol. **75:**7517–7527.

59. **Wang, F. Z., S. M. Akula, N. S. Walia, L. Zeng, and B. Chandran.** 2003. Human herpesvirus 8 envelope glycoprotein B mediates cell adhesion via its RGD sequence. J. Virol. **77:**3131–3147.

60. **Zarate, I. B. O., K. Kaelin, and F. Rozenberg.** 2004. Effects of mutations in the cytoplasmic domain of herpes simplex virus type 1 glycoprotein B on intracellular transport and infectivity. J. Virol. **78:**1540–1551.

61. **Zhong, W., H. Wang, B. Herndier, and D. Ganem.** 1996. Restricted expression of Kaposi sarcoma-associated herpesvirus (human herpesvirus 8) genes in Kaposi sarcoma. Proc. Natl. Acad. Sci. USA **93:**6641–6646.

62. **Zhou, F. C., Y. J. Zhang, J. H. Deng, X. P. Wang, H. Y. Pan, E. Hettler, and S. J. Gao.** 2002. Efficient infection by a recombinant Kaposi's sarcoma-associated herpesvirus cloned in a bacterial artificial chromosome: application for genetic analysis. J. Virol. **76:**6185–6196.

63. **Zhu, L., V. Puri, and B. Chandran.** 1999. Characterization of human herpesvirus-8 8-K8.1A/B glycoproteins by monoclonal antibodies. Virology **262:**237–249.